Drosophila Undigested Metabolite Profiling reveals age related loss of intestinal amino acid transport regulates longevity

Abigail A. Mornement, Rachael E. Dack, David P. Doupé, Rebecca I. Clark*

Department of Biosciences, Durham University, Durham, UK

*Corresponding author: rebecca.clark2@durham.ac.uk

Abstract

Age-related decline results in changes to the architecture of the intestinal epithelium and a loss of barrier function, accompanied by elevated stress and immune signalling and alterations to the intestinal microbial population. Interventions that prevent these phenotypes support longevity across several model organisms. Despite this we do not yet know whether age-related intestinal decline impacts nutrient management, a key function of the intestinal epithelium. Addressing this question is critical given that nutritional interventions hold significant promise in the development of anti-ageing therapies.

In this study we have developed *Drosophila* Undigested Metabolite Profiling (D.U.M.P.) to assess the impact of intestinal ageing on nutrient absorption/excretion balance. We demonstrate that ageing results in a significant increase in amino acid load in the intestinal lumen that shortens lifespan. While the microbiota contributes significantly to intestinal amino acid load, age-related increases remain in sterile flies and are associated with reduced expression of a subset of amino acid transporters. Knockdown of the amino acid transporter *slimfast* in the intestinal epithelium extends lifespan and confers improved microbial control in aged flies.

Our findings demonstrate that age-related intestinal decline may alter the capacity of the epithelium to take up nutrients, resulting in local changes to the nutritional environment that have consequences for health. We emphasise that diet is not the sole determinant of the intestinal nutritional environment, and that the status of the intestinal epithelium and its capacity for nutrient uptake is a key mediator in the response to dietary interventions. Therefore, further understanding the impact of intestinal ageing on nutrient management will be critical to the rational design of nutritional therapies.

Introduction

The ageing intestine has been the subject of intensive study in recent years with significant advances in our understanding of the molecular mechanisms that underpin intestinal homeostasis. Ageing results in a loss of intestinal epithelial homeostasis characterised by changes in architecture, cellular composition, and regenerative potential of the stem cells[1–5]. In addition, immune activation and intestinal permeability / barrier dysfunction increase and there are shifts in the size and taxonomic composition of the commensal microbiota[6–15]. These phenotypes are interrelated such that interventions that target one will impact other aspects of intestinal homeostasis. Moreover, preventing a loss of intestinal homeostasis with age delays age-related decline in the organism as a whole[3,6–8,14,16–21]. Collectively, these studies have established the importance of intestinal homeostasis as a cornerstone of healthy ageing.

Alongside these studies of intestinal cell biology, physiology and microbiota we have seen growing evidence of the role of nutrition in maintaining health throughout the life course. The signalling network that regulates metabolism and growth is well accepted to influence lifelong health. This network responds to nutritional cues, and dietary nutrients and feeding patterns can themselves regulate ageing (reviewed in Longo and Anderson, 2022[22]). It is clear from this body of work that interactions between nutritional cues and longevity-associated signalling pathways are complex and context dependent. Genetics, sex, existing health status and age of onset all influence the ability of dietary interventions to extend lifespan and improve health (reviewed in Longo and Anderson, 2022[22]). Despite the challenge posed by this complexity, personalised nutrition has the potential to optimise individual health and longevity.

One key outcome of the intensive study of nutritional regulation of ageing is an appreciation that nutritional needs change significantly with age[23] as does the ability of established nutritional interventions to extend longevity[22]. Taking this together with our knowledge of age-related intestinal decline it is surprising that few studies have addressed the impact of intestinal decline on nutrient management, a key function of the intestinal epithelium. In this regard, older animal studies suggest a reduction in transport of a range of nutrients with age[24–26]. More recently, it has been postulated that age-related defects in membrane trafficking drive loss of intestinal barrier function and might also disrupt nutrient

65 absorption, thus underlying age-related changes in metabolic status[27]. An assumption that
66 nutrient absorption is reduced with age pervades online sources of nutritional advice, and
67 while these claims are not unfounded it has not yet been established that a loss of nutrient
68 absorption is a general feature of ageing or whether such a loss impacts all nutrient types.
69 More importantly, the mechanisms underlying such a loss, the consequences for intestinal
70 physiology and ageing, and the impact on the effectiveness of nutritional interventions have
71 not been explored.
72 A recent article summarizing the discussions that took place at an NIH workshop on
73 diet and healthspan put forward a list of questions that will need to be considered priorities
74 in future research, among them the question: "Do nutrient transport and uptake change
75 with age?"[28]. However, exploring this is challenging because to date, tools enabling deeper
76 investigation of age-related changes in intestinal nutrient management have been limited.
77 We aim to address this in *Drosophila melanogaster*, a short-lived and genetically tractable
78 model system that has been extensively used in studies of the ageing intestine. We present
79 a novel assay that combines a chemically defined diet with metabolic profiling of faecal
80 nutrient content to assess changes in nutrient uptake/excretion balance with age. Using this
81 assay, we demonstrate that amino acid uptake is reduced in aged flies, and this is associated
82 with reduced expression of a subset of amino acid transporters in the midgut epithelium.
83 Further, a diet mimicking the intestinal amino acid load of aged flies is detrimental to the
84 health of young flies. These data suggest that age-related decline may drive changes in
85 nutrient absorption capacity with further consequences for health. Therefore, our findings
86 have significant implications for the rational design of nutritional interventions that aim to
87 delay age-related decline.
88
89 **Results**
90
91 **Drosophila Undigested Metabolite Profiling (D.U.M.P)**
92 To measure changes in nutrient absorption/excretion balance we adopted a strategy of
93 comparing nutritional input and output by combining a chemically defined *Drosophila*
94 media[29,30] with mass spectrometry profiling of faecal nutrient content. We included a non-
95 absorbable food dye in the media to calculate the quantity of food ingested for each faecal
96 sample by measuring its dye content. This enabled direct comparison between nutrient

intake and output.

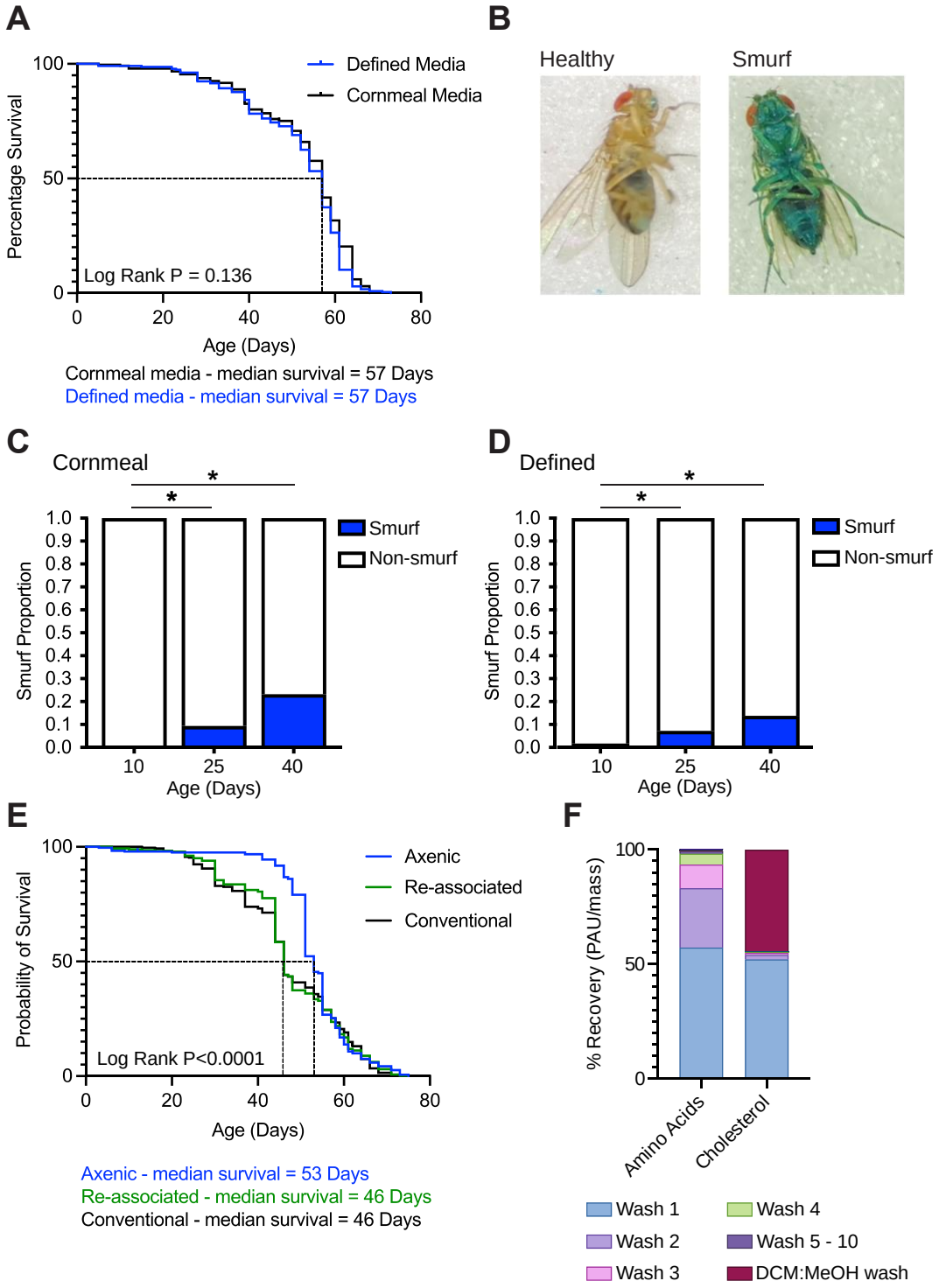

Supplemental figure 1. Defined media does not impact lifespan. (A) Lifespan of Canton-S female flies fed during adulthood on cornmeal or defined media. N > 200 per condition at day 1 (B) Images displaying the characteristic smurf phenotype. (C-D) Proportion of smurf flies within the total population taken at the ages shown for (C) cornmeal and (D) defined

media. N > 200 per condition at day 1 (E) Lifespan of axenic, re-associated and conventionally reared flies fed during adulthood on defined media. N > 450 Canton-S females per condition at day 1. Asterisks denote the result of binomial tests, where * $p<0.05$. (F) Percent recovery; the sum of percent abundance (PAU)/mass of all amino acids or cholesterol per wash, as a percentage of the sum of PAU/mass of all amino acids or cholesterol for all washes. No cholesterol was detected following wash 5.

First, we needed to establish that the defined diet supported the adult stage of our wild-type Canton-S flies as expected under our laboratory conditions. Given the previously reported developmental delay of flies reared on the defined diet[29], we reared flies on our standard cornmeal diet, transferring them to the defined diet in early adulthood. Diet is an important determinant of lifespan and age-related health and so we assessed the lifespan of our flies on the defined diet compared to our standard cornmeal diet. We found the change in diet did not alter the lifespan (Fig. S1A). We also found that flies on the defined diet continued to show an age-related increase in intestinal permeability (Fig. S1B-D) as measured by the Smurf assay[10,31]. Finally, we assessed the ability of the defined diet to support lifespan of axenic flies. We found axenic conditions resulted in lifespan extension (Fig. S1E), demonstrating that the nutritional requirements of adult female flies are fully met by the diet alone and do not need to be supplemented by the microbiota. In fact, the presence of the microbiota is detrimental with regards to lifespan in Canton-S females under our laboratory conditions.

Having confirmed the defined diet did not impact lifespan we developed a faecal collection protocol (Fig. 1A). Inclusion of FD&C blue no. 1 in the media enabled us to score “Smurf” flies that had lost intestinal barrier function and exclude them from the assay as the concentration of dye in the fecal matter is no longer representative of food intake [10,31]. In the remaining flies the concentration of blue no. 1 in each faecal sample then provides a proxy for food consumed. Normalisation of mass spectroscopy data to dye concentration controls for differences in food intake or the quantity of faecal matter collected.

For the purposes of this study, we quantified amino acids only from our final samples (see below); however, we provide details of sample preparation designed to enable

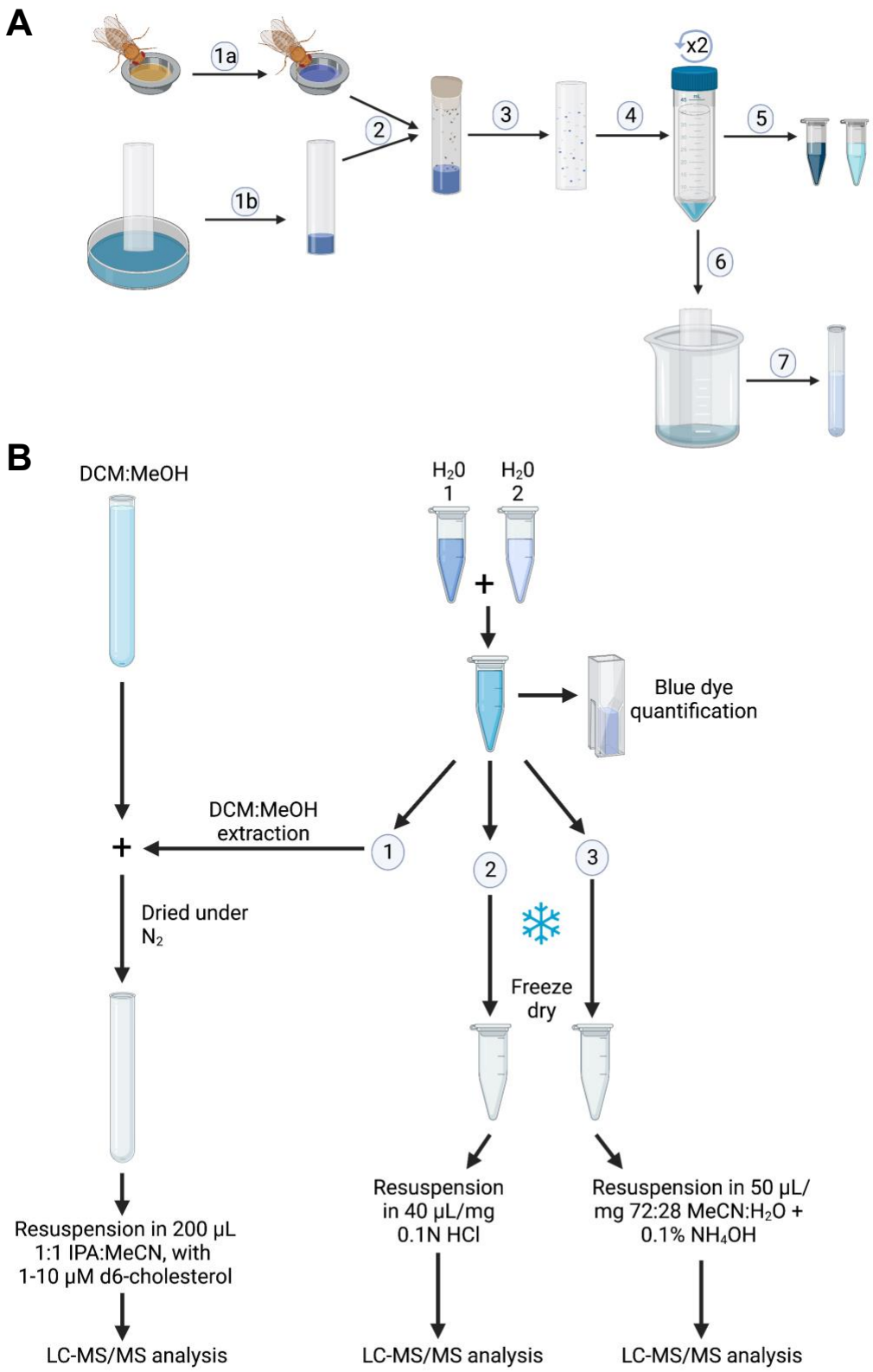

Figure 1. Schematic of Drosophila Undigested Metabolite Profiling assay. (A) Sample collection for the DUMP assay; 1a| Flies placed on blue food for 24h. 1b| Collection vials prepared. 2| 60 non-smurf flies transferred to collection tubes. 3| Flies incubated at 25°C for up to 5 hours, then anaesthetised and removed with food. 4| All collection vials washed

139 within falcon tubes with the same 1.5mL H_2O to produce a concentrated sample. Wash step
140 is repeated to give a second sample 5| water samples transferred to microfuge tubes and
141 stored at -80°C. 6| collection vials washed in 5mL 1:1 DCM:MeOH to collect non-polar
142 fraction. 7| DCM:MeOH sample collected in glass-storage tube. Sample stored upright at -
143 80°C. (B) Sample processing for the DUMP assay; the two water washes are combined and
144 1-2 µL removed for quantification of blue dye. The remainder is split three ways for 1.
145 Cholesterol, 2. Amino acid, and 3. Sugar analysis. DCM is added to the water fraction to
146 extract cholesterol. The DCM layer is added to the DCM:MeOH wash sample and dried
147 under a stream of N_2 before resuspension 1:1 IPA:MeCN. The amino acid and sugar samples
148 were lyophilised, then resuspended in 0.1N HCl or 72:28 MeCN:H_2O + 0.1% NH_4OH
149 respectively, prior to LC-MS/MS analysis. Full details of each step are given in the materials
150 and methods section.
151
152 measurement of amino acids, sugars and cholesterol from each faecal collection (Fig. 1B).
153 Faecal collection involved washing faecal matter from the sides of the collection vials. Initial
154 tests showed that two water washes were sufficient to collect 80% of amino acids and
155 almost 50% of cholesterol (Supp. Fig. 1F). Given the time required for each wash and the
156 diminishing returns from each additional wash, we used two water washes going forward.
157 An additional wash with DCM:MeOH enabled collection of the remaining cholesterol (Supp.
158 Fig. 1F), and presumably aids in collection of non-polar molecules more generally. We also
159 found the DCM:MeOH wash to contain some amino acids, including cysteine which was not
160 detected in the water washes. Together our faecal collection and analysis protocols result in
161 samples that can be used to measure a wide range of nutrients and metabolites. This
162 protocol can also be adapted for untargeted metabolomics approaches.
163
164 **Faecal amino acid levels increase with age**
165 Given the importance of dietary protein levels in lifespan determination[32] and previous
166 reports of reduced amino acid transport with age[24], we next applied the D.U.M.P. assay to
167 assess changes in amino acid absorption/excretion balance with age. We found a consistent
168 trend toward increased amino acid concentrations in faecal matter from aged flies, although
169 not every amino acid showed a statistically significant change (Fig. 2A).

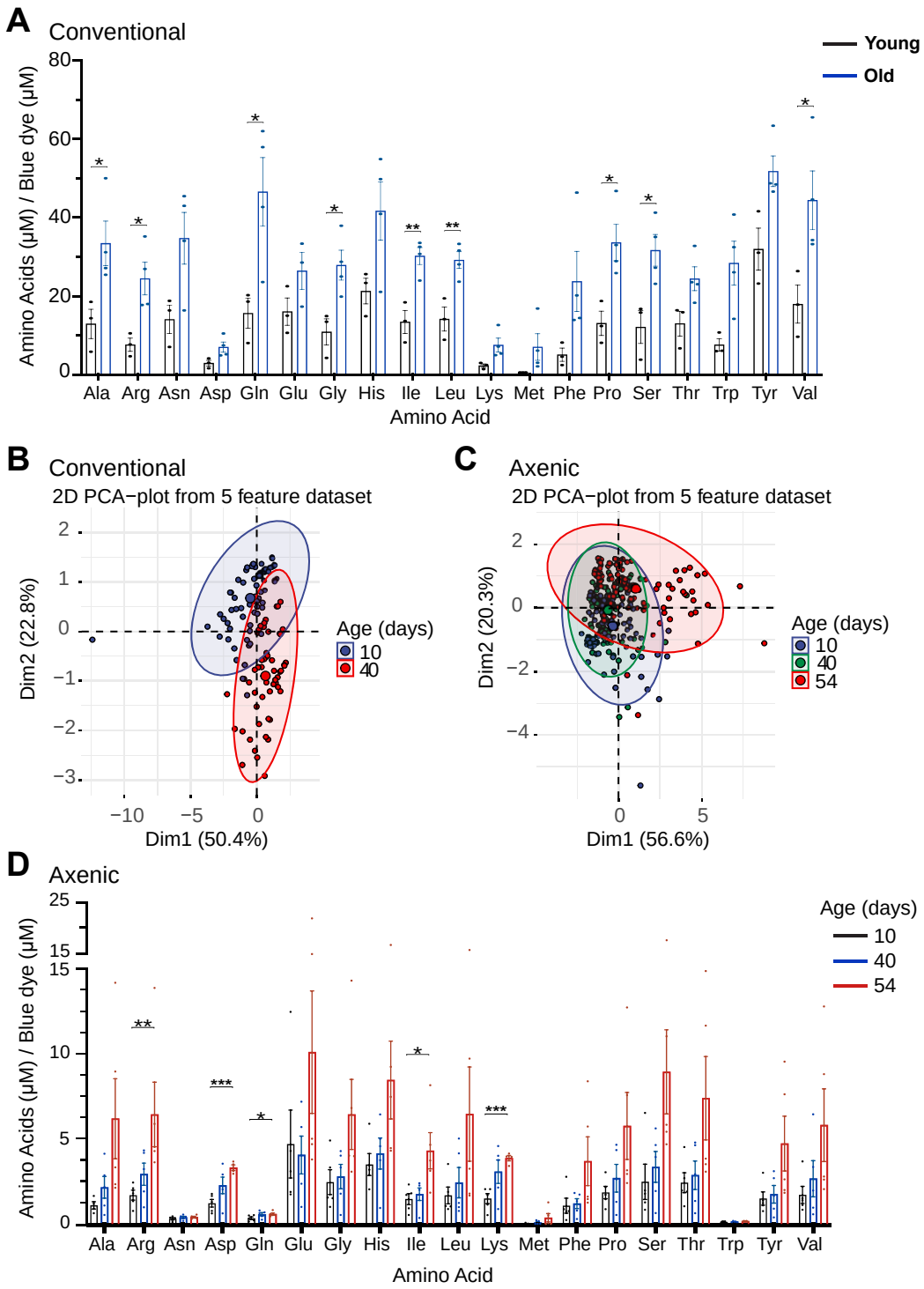

Figure 2: Drosophila Undigested Metabolite Profiling uncovers changes in nutrient egestion with age. (A) Relative concentration of amino acids in the faecal deposits of 10-day (9-11 day) and 40-day (39-44 day) flies, normalised to the concentration of blue food dye. (B-C) Principal component analysis for the overall structure of amino acid data from (B) conventional and (C) axenic samples plotted with respect to the first and second principal components. (D) Relative concentration in the faecal deposits of 10-day (9-11 day), 40-day

177 (38-40 day), and 54-day (52-54 day) axenic flies, normalised to the concentration of blue
178 food dye. Each sample pooled from >300 mated female Canton S flies. N = 3 biological
179 replicate samples for the conventional dataset and N = 5 for the axenic data. Bar graph
180 shows mean ± SEM. Asterisks denote the results of 2-tailed unpaired T-test (normally-
181 distributed data) or Mann-Whitney test (not-normally distributed data; (A) Trp and Try, (D)
182 Arg, Glu, Met, Phe, Ser and Val), where * P<0.05, **P<0.01, ***P<0.001. For the axenic data
183 tests compared 10- and 54-day samples.
184
185 We reasoned the previously reported age-related increases in microbial load in the
186 fly intestine[6,7,10,14] may drive this age-related increase in faecal amino acid concentrations.
187 To test the microbial contribution to age related changes, we repeated the D.U.M.P. assay in
188 a cohort of axenic flies. Given the lifespan extension seen in axenic flies we included a later
189 life faecal collection. To characterise the structure of the data we performed a principal
190 component analysis (PCA) on the conventional and axenic datasets. Plotting the data in
191 respect to the first and second principal components, which explain the most variance,
192 showed clustering by age in the conventional dataset (Fig. 2B). In the axenic dataset there
193 was no separation between the 10 and 40-day faecal samples, indicating a high degree of
194 similarity between these samples. However, the sample collected at 52-days shows
195 separation from the 10 and 40-day samples (Fig. 2C). This is consistent with the fact that the
196 axenic lifespan shows no increase in mortality at the 40-day timepoint, while the
197 conventional lifespan is at 75% survival at 40 days (Supp. Fig. 1E). The axenic lifespan drops
198 rapidly from 80% to 50% survival between days 50 and 53 (Supp. Fig. 1E), suggesting the 52-
199 day timepoint is a closer match to the 40-day conventional sample with regards to biological
200 age. For this reason, the 52-day sample was used for further analysis.
201 To determine the contribution of epithelial ageing to the changing faecal amino acid
202 profile in the absence of the microbiota we compared our axenic samples across the age
203 range. As suggested by our PCA analysis (Fig. 2C), a trend toward increased amino acid
204 concentrations in the faecal matter of aged flies remained in the axenic cohort, although
205 this was statistically significant for fewer amino acids than in the conventional dataset (Fig.
206 2D). The amino acids that showed statistically significant changes upon ageing were
207 different between the conventional and axenic datasets, demonstrating the contribution of
208 the microbiota. Nevertheless, age-related changes in the intestinal epithelium are sufficient

to result in changes in the faecal amino acid profile with age and in general contribute to an increased amino acid load in aged fly faeces.

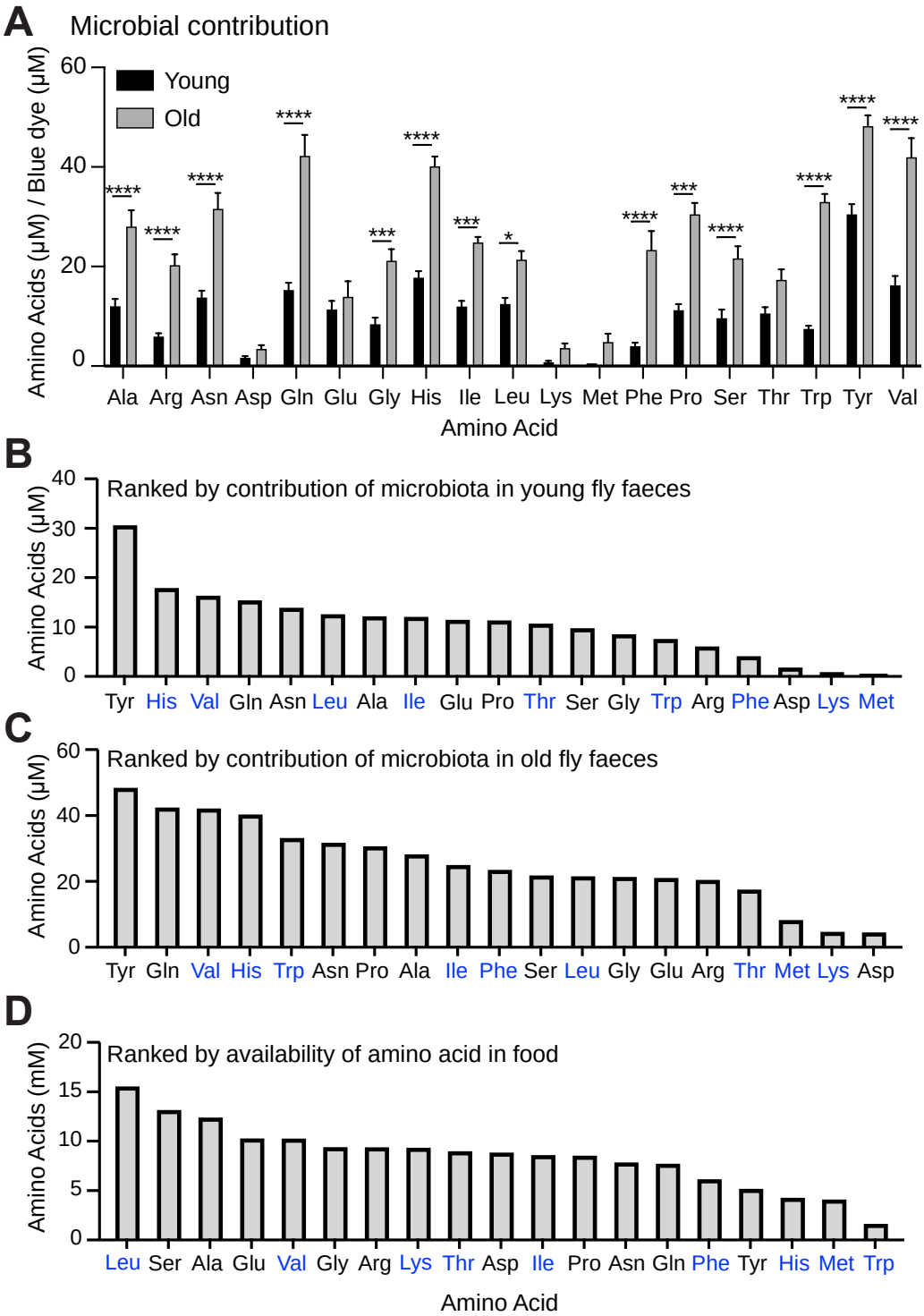

Supplemental figure 2: Microbial contribution with age shifts faecal amino acid profile. (A) Concentration of faecal amino acids, normalised to the concentration of blue food dye, contributed by the microbiota in young and old flies. The microbial contribution was

216 calculated for each amino acid at the young timepoint by; Conventional concentration (9-11
217 days) – axenic concentration (9-11 days), and at the old timepoint by; Conventional
218 concentration (38-40 days) – axenic concentration (52-54 days), using the concentration of
219 amino acid normalised to blue dye for each sample. For each amino acid, at each time point,
220 the calculation was carried out between every conventional and every axenic measurement.
221 (B-D) Amino acids ordered by level of microbial contribution in (B) young and (C) old flies,
222 and by (D) availability within the food. Blue amino acid labels denote essential amino acids.
223 Bar graph shows mean ± SEM. Asterisks denote the results of a 2-way Anova, where *
224 P<0.05, **P<0.01, *** P<0.001, ****P<0.0001
225
226 Although changes in faecal amino acid profile are observed in axenic flies a detailed
227 analysis of individual amino acid changes reveals important contributions from the
228 microbiota. Overall, the level of each amino acid is lower in axenic fecal matter compared to
229 conventional (Fig. 2A and D). To further assess this, we calculated the amino acid
230 concentration contributed by the microbiota in young (10-day conventional – 10-day axenic)
231 and old (40-day conventional – 52-day axenic) flies. This calculation was performed by
232 comparing every conventional value to every axenic value, for each amino acid. This analysis
233 confirmed that the microbiota is an important contributor to the faecal amino acid profile in
234 both young and old flies (Supp. Fig. 2A). To visualise age-related changes in microbial
235 contribution we ordered the amino acids by microbial contribution. Several changes in
236 graph position are seen between young (Supp. Fig. 2B) and old (Supp. Fig. 2C) flies,
237 confirming that changes in the microbial population contribute to age-related changes in
238 the faecal amino acid profile. In addition, the order of amino acids in both young and old
239 samples are different from that in the media (Supp. Fig. 2D), confirming the overall
240 contribution of the microbiota to the faecal amino acid pool.
241
242 **Recapitulating aged amino acid load shortens lifespan**
243 Given the elevation of amino acid levels in the aged intestinal lumen we next assessed
244 whether these changes altered lifespan. We used the D.U.M.P data to design a diet that
245 mimics the amino acid changes that occur with age in conventionally reared flies. The amino
246 acid concentrations in this diet, called Aged Amino Acid (AA) media, were determined by
247 adding the difference in mean concentration between the 10- and 40-day conventional

248 faecal samples to the concentration in the original defined media. Amino acid
249 concentrations in the Aged AA media ranged from 1.15 to 5.18 times the concentrations in
250 the standard defined diet. The average increase in concentration was 2.15 times that of the
251 standard diet, equivalent to dietary protein levels that have previously been shown to
252 reduce *Drosophila* lifespan[33].
253

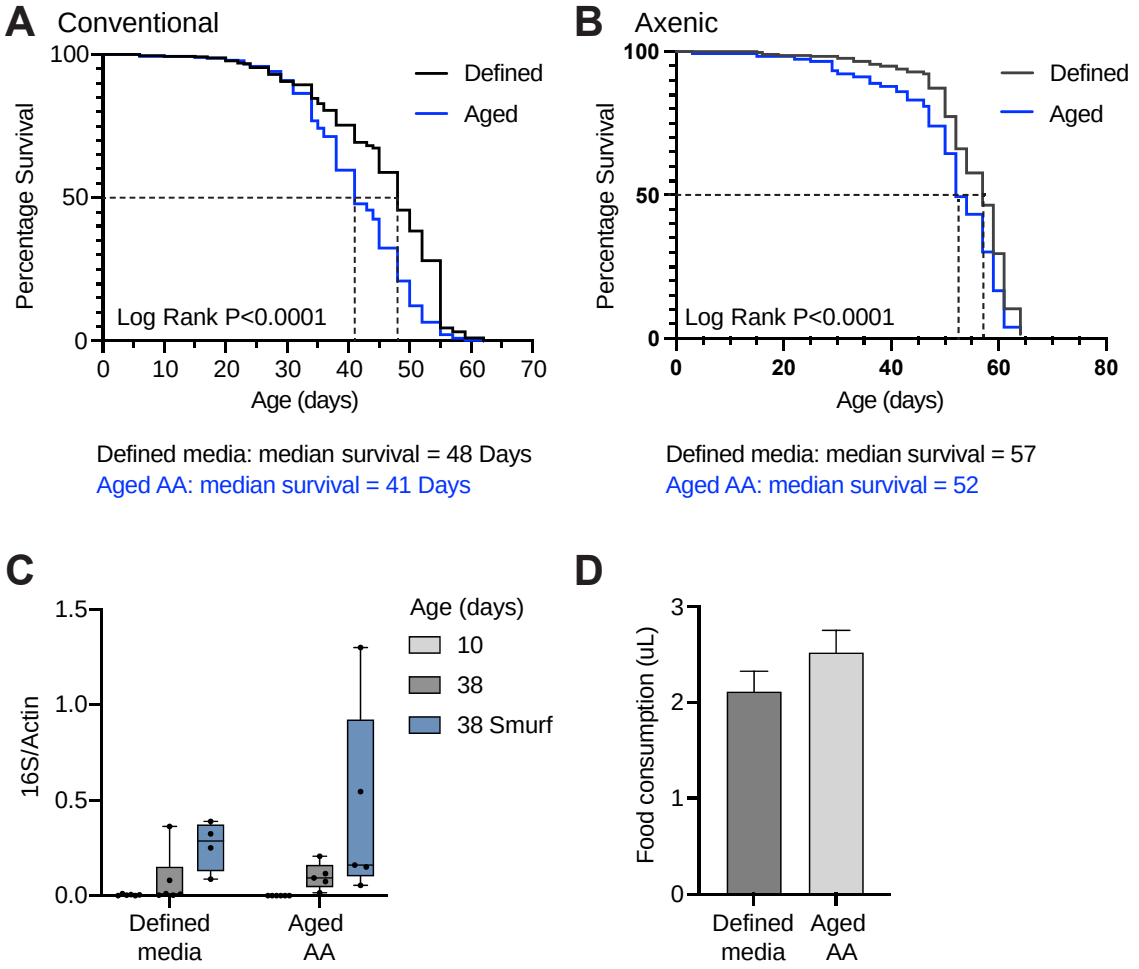

254

255 **Figure 3: Aged AA media reduced lifespan independent of microbial status.**
256 (A) Lifespan of conventionally colonised flies on defined media or Aged AA media. Dashed
257 black line denotes the median survival, n > 240 flies per condition at day 1. (B) Lifespan of
258 axenic flies on defined media or Aged AA media, n > 240 flies per condition at day 1. (C)
259 Internal bacterial load of young (10 day), old (38 day) and old smurf (38 days with intestinal
260 barrier dysfunction) flies measured using universal primers for the 16s rRNA gene,
261 normalised to actin. Data from at least 5 flies/sample, with a minimum of 6 samples. Box
262 plots show the 25-75th percentiles and the median with the whiskers extending from min-
263 max. (D) 48-hour food consumption (µL) of 9-10 groups of 10 flies fed liquid defined media

or Aged AA media (omitting cholesterol). Bars show mean and standard error. No significant difference by unpaired t-test. All experiments were performed on mated Canton-S female flies.

We found that exposure to the Aged AA media from young adult life significantly and reproducibly reduced lifespan (Fig. 3A, supp. Fig. 3A). This result was also observed in a cohort of axenic flies, suggesting it is independent of the microbiota (Fig. 3B). Consistent with this observation we found no significant impact of diet on internal bacterial load (Fig. 3C). In addition, a capillary feeding assay[34], showed no significant difference in food intake between the standard and Aged AA media (Fig. 3D). These data are consistent with the known lifespan impact of a high protein diet[32] and suggest that increased intestinal amino acid load may contribute to age-related decline.

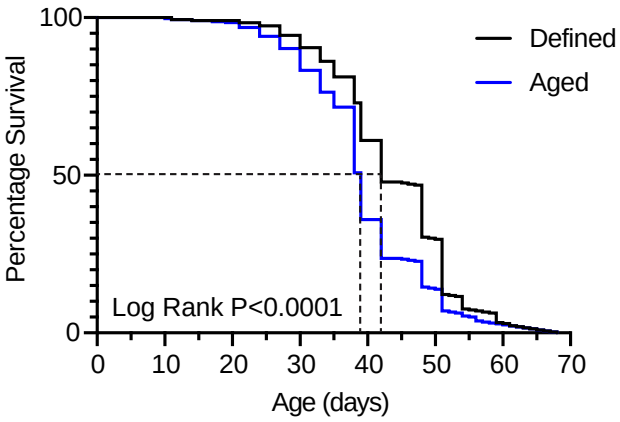

Defined media: median survival = 42 Days
Aged AA: median survival = 39 Days

Supplemental Figure 3: Aged AA media reduced lifespan

An independent replicate lifespan of conventionally colonised mated Canton-S females on defined media or Aged AA media. Dashed black line denotes the median survival, n > 240 flies per condition at day 1.

Expression of intestinal amino acid transporters changes with age

We next sought to understand why epithelial ageing results in increased faecal amino acid levels in the absence of the microbiota. We reasoned that this may reflect reduced amino acid transport across the intestinal epithelium with age, as previously reported for several

287 animal species[24]. As a proxy measure of transport capacity, we assessed the expression
288 levels of a panel of amino acid transporters in young and old intestinal tissue.
289 First, we generated a list of validated and predicted Drosophila amino acid
290 transporters; this list contained 48 genes, 21 of which were unnamed. To select for genes
291 expressed in the gut, we used the online databases Flygut-*seq*[35] and FlyAtlas 2[36]. Genes
292 which showed homology to human intestinal amino acid transporters were also identified
293 using DIOPT Ortholog Finder and included[37,38]. This generated a final list of 18 genes
294 spanning 8 solute carrier families (Supp. Table 1). Of these we were able to validate
295 quantitative PCR (qPCR) primers for 13 transporters, representing six solute carrier (SLC)
296 families (Supp. Table 1). The validated primers were were used to quantify expression in
297 young (10 day) and old (45 day) Canton-S female intestinal samples (Fig 4, supp. Fig 4).
298
299 **Supplemental Table 1:** Final list of genes with validated or predicted amino acid transporter
300 function and predicted intestinal expression. Top human orthologs and weighted DIOPT
301 score determined from https://www.flyrnai.org/cgi-bin/DRSC_orthologs.pl. The genes in
302 grey font were not taken forward due to poor qPCR primers. *All top orthologs, sharing the
303 same weighted DIOPT score.

Drosophila Gene	Annotation Symbol	Homologous human Solute carrier family	Top Human ortholog	Weighted DIOPT score
Eaat1	CG3747	SLC1	SLC1A3	9.85
CD98hc	CG2791	SLC3	SLC3A2	5.82
CG1698	CG1698	SLC6	SLC6A16	3.94
Naat1	CG3252	SLC6	SLC6A16	3.94
CG13796	CG13796	SLC6	SLC6A14	3.94
Slimfast	CG11128	SLC7	SLC7A1	12.84
CG5535	CG5535	SLC7	SLC7A1	10.92
CG7255	CG7255	SLC7	SLC7A2	8.75
Minidiscs	CG3297	SLC7	SLC7A7	8.88
Sobremesa	CG9413	SLC7	SLC7A9	13.75
Kazachoc	CG5594	SLC12	SLC12A4	14.75
dmGlut	CG5305	SLC17	SLC17A3	5.89
CG43693	CG43693	SLC36	SLC36A1	9.9
Pathetic	CG3234	SLC36	SLC36A1-4*	5.92
CG8785	CG8785	SLC36	SLC36A4	7.87
CG1139	CG1139	SLC36	SLC36A1-4*	6.85
CG30394	CG30394	SLC38	SLC38A10	10.73

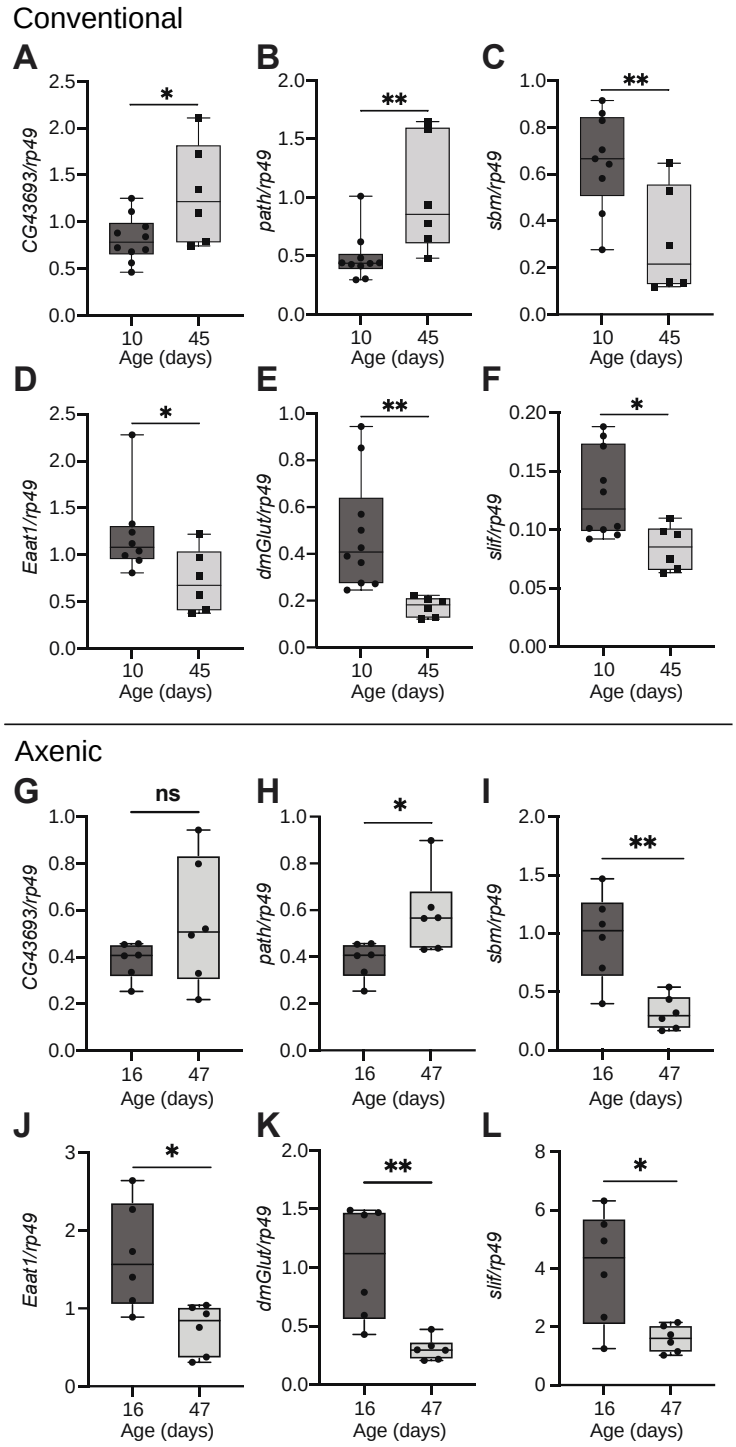

Figure 4: Age-related changes in amino acid transporter expression. (A-F) Transporter levels measured in dissected midguts from conventionally reared Canton-S females at 10 and 45 days of age. Normalised to the expression of rp49. N = 5 guts per sample, 8-10 samples at day 10, and 5-6 samples at day 45. (A) *CG43693*, (B) *Pathetic (path)*, (C) *sobremesa (sbm)*, (D) *Excitatory amino acid transporter 1 (Eaat1)*, (E) *dietary and metabolic glutamate transporter (dmGlut)*, (F) *Slimfast (Slif)*. (G-L) Transporter levels measured in dissected midguts from axenic Canton-S females at 16 and 47 days of age. Normalised to the

312 expression of rp49. N = 5 guts per sample, 5-6 samples at each timepoint. (G) *CG43693*, (H)
313 *Pathetic (path)*, (I) *sobremesa (sbm)*, (J) *Excitatory amino acid transporter 1 (Eaat1)*, (K)
314 *dietary and metabolic glutamate transporter (dmGlut)*, (L) *Slimfast (Slif)*. Box plots show the
315 25-75th percentiles and the median with the whiskers extending from min-max. Asterisks
316 denote the results of 2-tailed unpaired T-test (normally-distributed data) or Mann-Whitney
317 test (not-normally distributed data as calculated by the Shapiro-Wilk test; *path* and *Eaat1*
318 from conventionally reared flies (B,D)), where ns – not significant, * P<0.05, **P<0.01.
319
320 We found six transporter genes across 4 SLC families that showed statistically
321 significant changes with age: sbm, Eaat1, dmGlut and slif showed significant
322 downregulation, while CG43693 and path were upregulated (Fig 4). The amino acid
323 substrates for CG43693 (Fig. 4A) and Sombremesa (sbm) (Fig. 4C) are unknown, and
324 Pathetic (Path) (Fig. 4B) has been suggested to act primarily as a transceptor due to its low
325 transport capacity[39]. However, several amino acid transporters showed decreased
326 expression levels in aged intestines consistent with the D.U.M.P data.
327 Excitatory amino acid transporter 1 (Eaat1) (Fig. 4D) transports L-glutamate with
328 highest affinity, although L- and D- aspartate are also substrates, and there is evidence to
329 indicate a functional role in the intestine[40]. A second glutamate transporter, dietary and
330 metabolic glutamate transporter (dmGlut), also showed reduced expression with age (Fig.
331 4E). Both glutamate and aspartate show a trend toward increased levels in faecal samples
332 from old conventionally reared and axenic flies. This increase is statistically significant for
333 aspartate in axenic samples, suggesting the underlying cause is independent of the
334 microbiota.
335 Slimfast (slif) (Fig. 4F) transports L-arginine[41] and could be inferred to also transport
336 lysine due to its homology to the cationic amino acid transporter family, although this has
337 not been tested to our knowledge. A statistically significant increase in arginine and lysine
338 levels is seen in faecal samples from old axenic flies and for arginine in faecal samples from
339 old conventionally reared flies.
340 We further confirmed that the changes in expression reported for *path, sbm, Eaat1,*
341 *dmGlut* and *slif* were retained in axenic flies (Fig. 4H-K). CG43693 showed a trend toward
342 increased expression in old axenic flies, but this did not reach statistical significance. Overall,
343 this suggests the recorded changes in transporter expression are independent of the

microbiota. Taken together these data support a model whereby age-related changes in the expression levels of amino acid transporters result in reduced transport across aged intestinal epithelia and contribute to increased luminal amino acid levels.

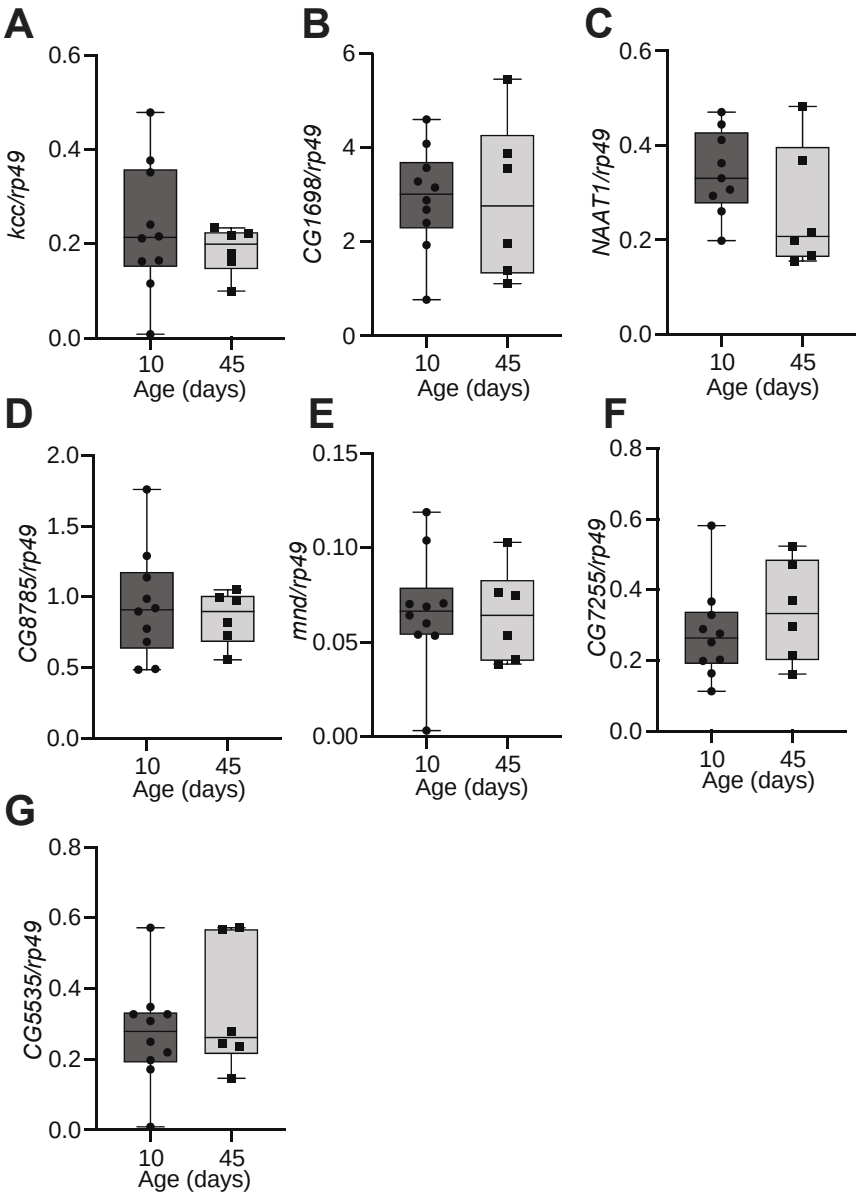

Supplemental Figure 4: Some amino acid transporters do not show changes in expression with age. Transporter levels measured in dissected midguts from conventionally reared Canton-S females at 10 and 45 days of age. Normalised to the expression of rp49. N = 5 guts per sample, 8-10 samples at day 10, and 5-6 samples at day 45. (A) *kazachoch (kcc),* (B) *CG1698*, (C) *Nutrient amino acid transporter 1 (Naat1),* (D) *CG8785,* (E) *minidiscs (mnd),* (F) *CG7255,* and (G) *CG5535.* Box plots show the 25-75th percentiles and the median with the whiskers extending from min-max.

356

357 **Intestinal slimfast expression level regulates lifespan**

358 We next sought to understand the physiological impact of reduced amino acid transporter

359 expression during ageing. We focused on slimfast due to the availability of genetic tools and

360 the significantly increased faecal concentration of its substrates with age.

361

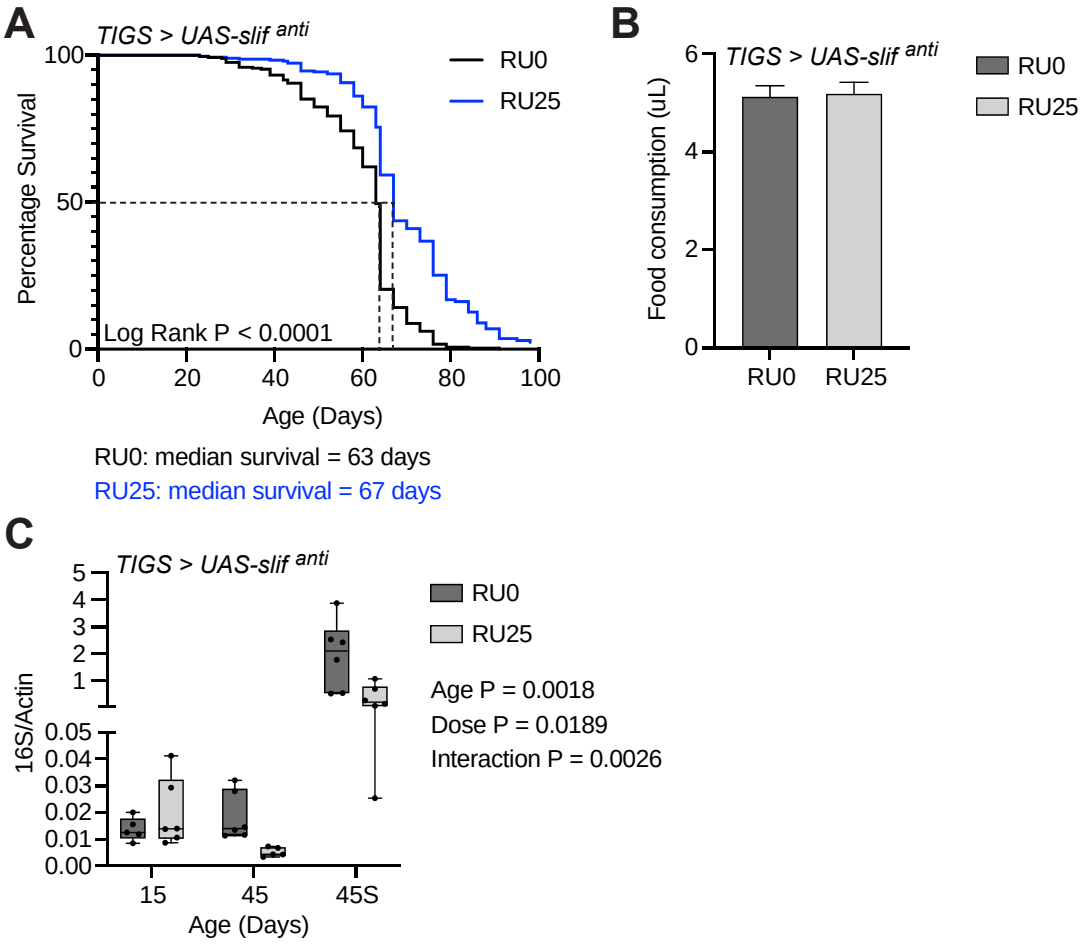

362

363 **Figure 5: Intestinal *slimfast* levels regulate lifespan.**

364 (A) Lifespan of *TIGS > UAS-Slif*^{anti} females on defined media with ethanol (RU0; black), or

365 25uM RU-486 (RU25; blue) throughout adult life. Dashed black line denotes the median

366 survival. (B) 48-hour food consumption (uL) of 6 groups of 10 *TIGS > UAS-Slif*^{anti} females fed

367 liquid defined media (omitting cholesterol) for 48 hours, following 72h induction of

368 knockdown (RU25) or control (RU0) treatment. (C) Internal bacterial load of 15 and 45 day

369 old, and 45-day old Smurf (45S) *TIGS > UAS-Slif*^{anti} females, with and without induction of

370 intestinal *Slif* knockdown. Conventionally colonised mated females are used throughout. Bar

371 graphs show mean and standard error. No significant difference by unpaired t-test. Box

372 plots show the 25-75th percentiles and the median with the whiskers extending from min-
373 max. Two-way Anova with Tukey's multiple comparisons P-values are shown below key in
374 panel C.
375

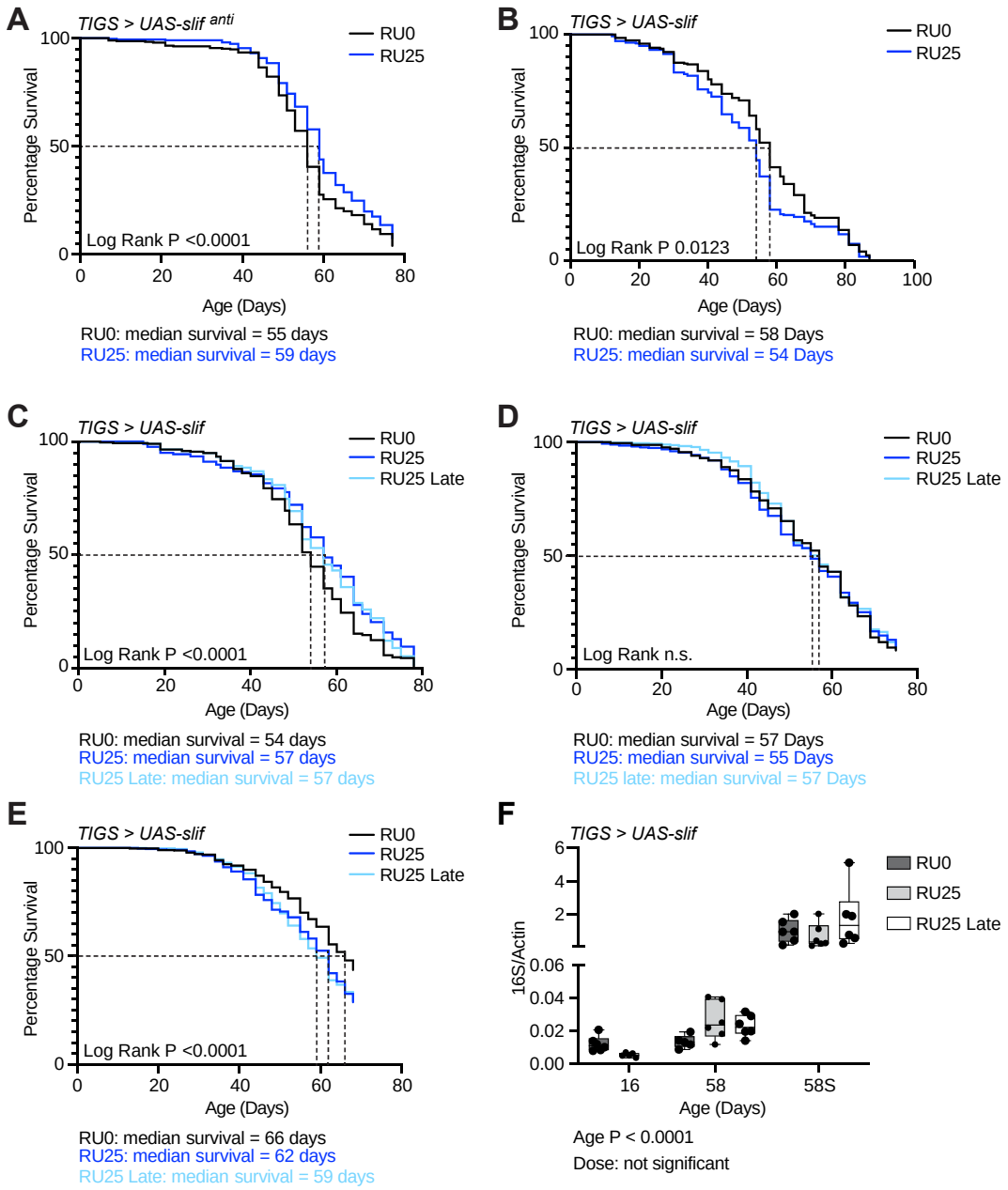

376

377 **Supplemental Figure 5: Intestinal *slimfast* levels regulate lifespan.**

378 (A) Replicate lifespan of conventionally colonised mated *TIGS > UAS-slif*^{anti} females on
379 defined media with ethanol (RU0; black), or 25uM Ru-486 (RU25; blue) throughout adult
380 life. Dashed black line denotes the median survival. (B-E) Replicate lifespans of
381 conventionally colonised mated *TIGS > UAS-slif* females on defined media with ethanol
382 (RU0; black), 25uM Ru-486 throughout adult life (RU25; dark blue) or from day 35 (RU25

383 late, pale blue). Dashed black line denotes the median survival. (F) Internal bacterial load of
384 16 and 58 day old, and 58-day old Smurf flies (58S) mated female *TIGS > UAS-slif* females,
385 with induction of intestinal *slif* overexpression throughout adult lifespan (RU25) or from day
386 35 (Late RU25) and ethanol treated controls (RU0). Box plots show the 25-75th percentiles
387 and the median with the whiskers extending from min-max. Two-way Anova with Tukey's
388 multiple comparisons P-values are shown below graph in panel F.
389
390 To determine whether the age-related loss of *slif* expression is functionally relevant,
391 we knocked down *slimfast* expression specifically in intestinal tissue from early adulthood.
392 We used the *slif-antisense* line ($slif^{anti}$)[41] and the TIGS driver, a drug inducible geneswitch
393 Gal4[42,43], enabling us to restrict knockdown to the adult stage. We observed a significant
394 and reproducible lifespan extension in drug induced females compared to vehicle controls
395 (Fig. 5A and Supp. Fig 5A). Given that slimfast has been previously shown to regulate
396 feeding[44,45] and that reduced food intake itself can regulate lifespan we performed a
397 capillary feeding assay[34]. We found no observable difference in the volume of food
398 consumed (Fig. 5B). Considering that reduced intestinal *slif* may alter luminal nutrient
399 availability,
400 subsequently altering the intestinal microbiota, we measured bacterial load using qPCR of
401 the bacterial 16S gene. Interestingly, we observed reduced bacterial load in old $slif^{anti}$
402 females (Fig. 5C), both prior to and following loss of intestinal barrier function. In contrast,
403 overexpression of *slif* in the intestine for the full adult lifespan or during later adult life had
404 no consistent impact on lifespan and did not change intestinal bacterial load (Supp. Fig. 5B-
405 F). These data suggest loss of intestinal *slif* expression in later life may be protective and
406 may confer improved control of the intestinal microbiota in the aged intestine.
407
408 **Discussion**
409 In this study we have developed a powerful new assay that enables us to investigate the
410 relationship between intestinal homeostasis and nutrient management in a genetically
411 tractable model system. We have used the D.U.M.P assay to demonstrate an increase in
412 amino acid levels in the faecal matter, and by proxy the intestinal lumen, of aged flies. It is
413 important to note that our targeted mass spectrometry approach measures only free amino
414 acids. Free amino acids in the faeces will include those remaining unabsorbed from the diet,

415 as well as those contributed by secretion from microbial or fly cells, and those released from
416 microbial or fly proteins by digestion. Comparison between the faecal content of
417 conventional and axenically reared flies has demonstrated the significant contribution of the
418 intestinal microbiota to the luminal amino acid pool. It also demonstrates the significant
419 changes in this contribution that result from age-related shifts in the microbial population.
420 How changes to microbial load and taxonomic representation in the aged intestinal
421 microbiota impacts the local nutritional environment and reciprocally how the local
422 nutritional environment impacts the microbiota warrant further investigation.
423 In addition to the microbial contribution, secreted proteins and shed fly cells may
424 contribute to the nutrient pool. Elevated immune responses in the aged intestine could
425 raise both the levels of secreted proteins (including antimicrobial peptides and other
426 immune responsive proteins) and intestinal cell death and shedding[6,7,46,47]. Our current data
427 cannot distinguish between amino acids remaining unabsorbed from the diet and those
428 contributed from secreted fly proteins or shed intestinal cells. However, it will be important
429 to address the relative contributions of these amino acid sources in future studies. Reduced
430 expression levels of a subset of amino acid transporters in the aged intestine suggests that
431 reduced amino acid transport into epithelial cells also contributes to elevated luminal levels
432 in aged animals. While past studies have focused on the importance of dietary protein levels
433 to healthy ageing (reviewed in Babygirija and Lamming, 2021[32]), our data highlight
434 additional sources of elevated amino acid exposure in the aged intestine. Could reductions
435 in dietary protein levels be effective in improving health because they counter natural
436 increases in amino acid exposure that result from age-related intestinal decline?
437 As we would expect from previous studies[32], increasing dietary amino acid levels
438 shortens lifespan. It is important to note that when feeding additional amino acids to young
439 flies we assume an increased uptake of amino acids by the intestine, and therefore elevated
440 amino acid levels in intestinal cells and other tissues. However, reduced transport of some
441 amino acids by the aged intestine would mean that in older individuals elevating dietary
442 amino acid levels may not result in elevated levels of all amino acids in the intestinal cells or
443 other tissues, with potential consequences for metabolic status. Therefore, it is important to
444 distinguish between the impacts of distinct amino acid pools, those that remain in the gut
445 lumen and those that undergo transport into the organism. This is evidenced in our data,
446 given that knockdown of *slimfast* can be expected to raise luminal levels of the amino acids

447 that it transports but, contrary to the impact of increased dietary amino acids, extends
448 lifespan.
449 There is some evidence that increased levels of *slimfast* substrates may be beneficial
450 to gut health. Arginine has been shown to improve intestinal immunity phenotypes in mice,
451 through modulation of the microbiota[48]. Increasing arginine levels also increases the
452 diversity of murine microbiota[49,50] improving the phenotypes of a colitis model[49]. The
453 benefits can also be passed on through faecal transplantation, whereas antibiotic treatment
454 prevents the improved colitis phenotypes[49,51]. Supplementation of lysine in lambs has also
455 been shown to protect intestinal mucosa and integrity, enhance innate immune responses,
456 and alter microbial composition[52]. It is unknown whether the benefits of supplementing
457 with these amino acids requires their uptake by intestinal cells, or whether elevated levels in
458 the gut lumen is sufficient. The impact of elevated levels of *slimfast* substrates on the
459 microbiota may be reflected in the improved microbial control that we record following
460 *slimfast* knockdown.
461 In addition to impacts on the microbiota, some amino acids may have specific roles
462 in maintaining health of the intestinal epithelium. For example, increased glutamate
463 concentration has been shown to stimulate intestinal stem cell (ISC) proliferation in
464 *Drosophila*[40] and in mice[53]. Interestingly, whether proliferation was impaired or stimulated
465 depended on glutamate concentration[40]. L-arginine has also been shown to stimulate ISC
466 expansion in mice[54]. Elevated activity of the amino acid sensing Target of Rapamycin (TOR)
467 pathway, an established regulator of longevity, as a result of elevated amino acid levels may
468 also have a role in intestinal decline. Recently, it has been demonstrated that TOR inhibition
469 delays age-related intestinal decline[4,55–58] with genetic interventions targeted to intestinal
470 stem cells sufficient to preserve homeostasis[4,58]. Evidence is also emerging that elevated
471 TOR activation in intestinal cells may be a feature of natural ageing[4,59]. The impact of
472 reduced *slimfast* levels on larval growth is mediated by reduced TOR activity[41], and we
473 suggest that reduced *slimfast* levels in the gut may protect against elevated luminal amino
474 acid levels via reduced TOR activity.
475 Substrates of *slimfast* also have roles beyond the gut. Reduced levels of arginine and
476 lysine are associated with ageing skeletal muscle[60], while arginine and lysine have been
477 shown to have a positive association with lifespan in a study of fibroblasts taken from a
478 range of primate, avian and rodent species[61]. Lysine also decreases with age in *C. elegans*[62–

479 [64]. and supplementation of arginine or lysine increases the lifespan[65]. High lysine levels have
480 also been linked to longevity in humans[66]. Despite the evidence for the beneficial effects of
481 arginine in the gut, arginine supplementation has been shown to increase the secretion of
482 IGF-1[67] and growth hormone[68], both of which have pro-ageing functions in mice[69–71]. It also
483 stimulates activity of the TOR pathway[72]. Increased arginine levels have been found in aged
484 Drosophila[73] and supplementation of 20mM arginine to the diet of Drosophila leads to a
485 lifespan reduction, and reduced fecundity[74]. These apparent contradictions again suggest
486 pleiotropic roles for individual amino acids acting in metabolism and as signalling molecules
487 systemically and within individual tissues.

488 Moving forward it will be important to deepen our understanding of the impact of
489 intestinal ageing on the epithelium's ability to take up nutrients, the resulting changes to
490 the local nutrient environment and the apparent pleiotropic roles of individual nutrients.
491 Such understanding will be critical in the development of rationally designed nutritional
492 therapies. For example, despite the evidence to suggest a detrimental effect of high-protein
493 diets, there are currently calls to increase the daily recommended protein intake for elderly
494 persons to prevent or reduce age-related muscle loss and sarcopenia[75]. Aged muscle cells
495 are believed to be resistant to stimuli such that elderly individuals must consume higher
496 amounts of protein to stimulate muscle growth[76–78]. However, our data suggest reduced
497 amino acid uptake by the intestine may be an additional mechanism underlying reduced
498 muscle mass in the elderly. Perhaps higher quantities of protein must be consumed because
499 a lower proportion is absorbed and bioavailable to the muscles. Raising protein levels in the
500 intestinal lumen may counter reduced amino acid transport ability but may also hasten
501 intestinal decline.

502 In conclusion, our findings demonstrate that age-related decline impacts nutrient
503 management by the intestinal epithelium, which profoundly changes the local nutritional
504 environment with consequences for age-related health. While we have focused on one class
505 of nutrient and on the impact of intestinal ageing, the D.U.M.P. assay has much broader
506 applicability. In combination with the genetic tools available in *Drosophila* and the
507 tractability of the *Drosophila* microbiota, the D.U.M.P. assay will enable researchers in this
508 field to assess the impact of a wide range of perturbations on the gut nutrient pool. For
509 example, how does nutrient availability change during infection or following a loss of
510 cellular homeostasis and subsequent regeneration? What role does nutritional availability

511 play in these processes? In what ways do specific microbes contribute to the nutrient pool,
512 and how does this change following perturbation of the microbial community? How do
513 changes in the expression of nutrient transporters impact the nutrient pool, in what
514 circumstances beyond aging do these changes occur, and what are the consequences for
515 intestinal physiology, microbial balance and organismal health? Given that the local
516 nutritional environment is not simply determined by the diet, such studies are an essential
517 complement to efforts to understand the impact of the levels of specific nutrients on
518 intestinal homeostasis, metabolic status, and organismal health.
519
520 **Materials and Methods**
521
522 **Fly stocks**
523 This work used the wild-type Canton-S strain (gift of Linda Partridge), TIGS-2-GeneSwitch
524 driver line[79] (gift of David Walker), UAS-slif^{anti} (BDSC #52655) and UAS-slif (BDSC #52661).
525
526 **Fly culture**
527 Flies were maintained in either vials or bottles in incubators with 65% humidity and a 12-
528 hour light/dark cycle, at either 18°C or 25ºC. Stocks were maintained on cornmeal medium
529 comprised of 1 % agar (SLS, FLY1020), 3% dried inactivated yeast (Genesee Scientific, 62-
530 106), 1.9 % sucrose (Duchefa Biochemie, S0809), 3.8 % dextrose (Melford, G32040) and 9.1
531 % cornmeal (SLS, FLY1110), all given in wt/vol, and water at 90% of the final volume.
532 Preservatives; 10 % Nipagin (SLS, FLY1136) in ethanol and an acid mixture comprised of 4.15
533 % phosphoric acid (VWR, 20624.262) and 41.8 % propionic acid (Sigma, P5561) in water,
534 previously described by Lewis, 1960[80], were added following boiling.
535
536 **Defined media**
537 The standard defined medium was prepared as in Piper *et al*. 2014[29] using the suggested
538 addition of 50 % more vitamin solution and the exome matched amino acid concentrations
539 'FLYAA' reported in Piper *et al.* 2017[30]. Contrary to the published method, buffer A
540 containing the metal ion solutions, low solubility amino acids, cholesterol, MilliQ water and
541 acetate buffer was brought to a boil in the microwave, not autoclaved at 121 ° C for 15
542 minutes, except in the preparation of sterile medium for axenic flies. The remaining

543 ingredients of essential and non-essential amino acid solutions, cysteine and glutamic acid
544 solutions, vitamin solution, lipid-related metabolite solution, folate, 10 % nipagin in ethanol,
545 and propionic acid were added once buffer A was cooled to 65 ° C, and thoroughly
546 incorporated. Aged AA media was prepared in the same way, but both the quantities of
547 amino acids used to make the stock solutions and the volume of stock solution used was
548 altered. The masses of amino acids added to the AA media were calculated by the
549 difference between mean old and mean young concentrations measured by the D.U.M.P.
550 assay in conventionally reared flies, plus the original defined media amino acid
551 concentration for each amino acid. Complete recipes for both the standard and Aged AA
552 media are given in a supplemental protocol file attached to this manuscript.
553
554 **Lifespan**
555 All experiments were carried out using age-matched mated females, housed at a density of
556 27-32 flies per vial. These flies were flipped onto new food within 24 hours of eclosing. They
557 were then allowed at least a further 24 hours to mate before the mated females were
558 sorted under light CO_2 anaesthesia into vials containing defined media at 48-96 hours after
559 eclosion. Flies were flipped to fresh food every 2-3 days and the number of dead flies was
560 counted. At least 6 vials of 30 females were used per lifespan. To control for bacterial
561 growth on the food, control and experimental flies are always transferred to fresh food at
562 the same time points.
563 Mifepristone or RU-486 (Cayman chemicals, 10006317), hereafter referred to as RU,
564 food was prepared by the addition of 125 µL of 20 mg/ml RU stock solution per 100mL food.
565 To ensure sufficient volume for effective mixing 125 µL of RU stock was added to 125 µL of
566 100% ethanol per 100 mL of food prior to addition to the food. Control food was prepared
567 by the addition of 250 µL ethanol per 100 mL food. Food was mixed thoroughly to ensure a
568 homogenous solution.
569
570 **Smurf assay**
571 The smurf assay[31] for intestinal barrier integrity was performed by flipping flies onto food
572 containing 2.5 % FD&C blue food dye #1 for 24 hours (FastColours, 08BLU00201). After 24
573 hours, the flies were flipped back onto dye-free food and the number of 'smurf' and 'non-
574 smurf' flies were recorded.

575

576 **Generation of axenic and reassociated flies**

577 To generate sterile (axenic) flies, eggs were collected on apple juice agar plates seeded with
578 a paste of live bakers yeast and ddH_2O, then washed and treated with bleach and ethanol
579 as described previously[81]. All steps were carried out in a laminar flow hood. Briefly, <14
580 hour-old embryos were dechorionated in 2 % sodium hypochlorite solution for 2.5 minutes,
581 rinsed in 70 % ethanol for 5 minutes and then rinsed with ~200 mL sterile PBS. Embryos
582 were then resuspended in sterile 0.01 % PBSTx (PBS + 0.01 % Triton X-100 (Sigma, X100))
583 and transferred to sterile autoclaved cornmeal medium.

584 To re-associate sterilised embryos with parental gut bacteria, 100 µL adult fly
585 homogenate (1 fly/20 µL sterile PBS) was added to sterile cornmeal medium prior to
586 addition of axenic embryos and allowed to dry. Flies were surface sterilised for 5 minutes in
587 70 % ethanol prior to homogenisation to ensure only internal microbes were present in the
588 homogenate. Where conventionally reared flies were used as a further control to axenic or
589 re-associated flies, 30 mated females were placed in vials containing sterilised cornmeal
590 food and allowed to lay eggs for 24 hours, starting the evening prior to embryo collection.
591 All medium for sterile and control flies was sterilised by autoclaving for 15 minutes at 121
592 °C, and all equipment used to push flies was first sterilised in Virkon for at least 20 minutes,
593 then rinsed and stored in 80 % ethanol. Gas pads were subsequently dried by running CO_2
594 through them. To maintain sterility, axenic females were separated into lifespan vials next
595 to an open flame and flipped to new sterile food every 2-3 days in a laminar flow hood.

596 Sterile conditions were confirmed throughout lifespans by testing the sterility of
597 soiled vials. Soiled stoppers were pressed into single wells of 12-well plates (Starlab, E2996-
598 1610) containing 3 mL of pre-poured and set LB Miller Agar. The plates were incubated at 37
599 °C for 24-48 hours to check for bacterial growth.

600

601 **Drosophila Undigested Metabolite Profiling (D.U.M.P.) assay**

602

603 *Preparation*

604 This assay relies on knowing the full content of the defined media. To prepare, defined
605 media was cooked as described above, with the addition of 2.5 % blue food dye #1 after
606 cooking (as in the Smurf assay). As well as preparing 4 mL vials, the food was poured into

607 petri-dishes for the assembly of collection vials. Collection vials are open-ended glass tubes
608 with 2.4 cm external diameter and 9.6 cm high, similar dimensions to standard fly vials.
609 These were provided by the glassblowing workshop within the Durham University chemistry
610 department. Prior to beginning the assay, collection tubes were prepared by using each
611 tube to stamp out a disc of food from the prepared petri-dish. The food discs were secured
612 in place in the tube ends with parafilm. This plugs one end of the vial; the other end of the
613 tube was plugged with a foam Droso-Plug (SLS, FLY1000).
614 24 hours prior to sample collection, flies were flipped onto defined media containing 2.5 %
615 FD&C blue food dye #1. This ensures that the flies' guts will be full of the assay media
616 containing the dye for normalisation. Additionally, this is enough time for flies losing
617 intestinal barrier function to become clearly visible, enabling their exclusion from the assay.
618
619 *Sample collection*
620 To begin the assay, flies were sorted into the pre-prepared collection vials under light CO_2
621 anaesthesia. Approximately 55 - 65 non-smurf, mated females were sorted into each vial.
622 More flies do not increase the amount of faecal deposit as when overcrowded they get
623 stuck at the bottom of the vial. 6 collection vials were used per sample to ensure a large
624 enough sample for full analysis. Once the flies awoke from anaesthesia, they were
625 incubated at 25°C for between 4 and 5 hours to eat and defecate as usual. Standing the vials
626 at a 45° angle results in an improved sample, particularly when collecting samples from aged
627 flies with reduced mobility. Following incubation, the flies were anaesthetised with CO_2, the
628 parafilm removed and the food disc along with the flies was pushed out from the bottom of
629 the tube. The outside of the vial and the food residue was cleaned with a tissue dampened
630 by milliQ water until the tissue came away clean.
631 The collection vials were all the same weight (26.91g ± 0.41) and fit inside 50mL
632 falcon tubes. Once within the 50 mL tube, the collection vials were thoroughly rinsed with
633 1.5 mL of water to collect the polar, water-soluble faecal fraction, and spun down. The same
634 1.5 mL of water was used to rinse each tube. This ensured the sample could be frozen and
635 lyophilised quickly. Two falcon tubes are used, with the collection vials each being washed,
636 then the water sample split between the falcons, to ensure the tubes are balanced for
637 centrifugation. Once all tubes are rinsed, the sample is transferred to a microcentrifuge

638 tube. The rinse is repeated a second time to ensure all faecal matter is collected, resulting in
639 two water-wash samples of 1.5 mL.
640 The vials were then rinsed thoroughly with a 1:1 mixture of DCM and methanol to
641 collect non-polar deposits. The rinses were carried out in a small glass beaker to collect the
642 sample. The volume for this wash was not limited, but approximately 5 mL was used for all
643 the tubes. Plastic use should be avoided with the DCM:MeOH wash. All samples were frozen
644 at -80 ° C prior to downstream processing.
645
646 *Sample processing*
647 The two water washes were combined, and 1-2 μL was removed and diluted 1/100 for the
648 blue dye to be quantified at 628nm absorbance, on the Bio-tek Synergy H4, alongside a
649 standard curve of known concentration. The remaining sample was split three ways to
650 enable analyte-specific processing and quantification. While we only quantified amino acids
651 in our final samples for the purpose of this study, we provide details for initial processing of
652 the other sample types here. The amino acid and sugar fractions were lyophilised and
653 weighed, then resuspended in 40 μL 0.1N HCl, or 72:28 MeCN:H_2O + 0.1% NH_4CN per mg
654 respectively. The resuspended amino acid sample was diluted 1:100 in HILIC A for LC-MS/MS
655 analysis, and the sugar samples were diluted between 1:10 and 1:100 in the 72:28
656 MeCN:H_2O + 0.1% NH_4CN prior to LC-MS/MS analysis. The third fraction was for cholesterol
657 analysis. An equal volume of DCM was added to the water fraction, then the sample was
658 vortexed for 2 minutes prior to 15 minutes of centrifugation at 1000x rpm. The DCM layer
659 was removed and added to the DCM:MeOH wash, this was dried under a stream of N_2, then
660 resuspended in 200 μL 1:1 IPA:MeCN, and spiked with 10 μM d6-cholesterol prior to LC-
661 MS/MS analysis.
662
663 *Amino acid quantitation*
664 LC-MS/MS analysis was performed on a Shimadzu Nexera X2 Ultra-Fast Liquid
665 Chromatography system consisting of binary pumps, an on-line degassing unit, an
666 autosampler, and a column oven (Shimadzu Corporation, Kyoto, Japan), coupled with an AB
667 Sciex 6500 QTRAP mass spectrometer consisting of an electrospray ionization (ESI) source
668 (AB SCIEX, Framingham, MA, USA). 1uL of sample of injected on to a BEH Amide (1.0 x
669 100mm, Waters, Milford, MA, USA), BEH HILIC (1.0 x 100mm, Waters, Milford, MA, USA) or

670 Ascentis HILIC (2.1 x 150mm, Waters, Milford, MA, USA) maintained at 40 °C, at a flow rate
671 of 0.2 mL/min or 0.3mL/min for the 1.0 and 2.1mm columns respectively. Three columns
672 were used to enable separation of isomers leucine and isoleucine, and optimal peak shape
673 for more accurate quantification. The mobile phases consisted of Solution A (85% MeCN +
674 0.15% FA + 10mM ammonium formate) and Solution B (85% H_2) + 15% MeCN + 0.15% FA +
675 10mM ammonium formate). A gradient elution was optimized for the separation of amino
676 acids with 1.5 min equilibration 0-6.0 min, 0% Solution B; 6.0-10 min, 0-100% Solution B; 10-
677 12 min, 100% Solution B; 12-12.1 min, 0% Solution B; 12.1-18 min, 0% Solution B; with a
678 total run time of 21 min. The ion source was operated in positive mode under an optimal
679 condition: curtain gas, 40 psi; nebulizer gas, 50 psi; auxiliary gas, 50 psi; ion spray voltage,
680 5500 V; and temperature, 500°C. Optimal multiple-reaction monitoring (MRM) transitions
681 were identified for the amino acids (Supplemental table 2). Quantification was performed
682 using an external calibration curve, amino acids stocks in 0.1N HCl were diluted with HILIC A
683 as per sample preparation. Data acquisition and analysis were all performed with Analyst
684 1.6.3 software (AB SCIEX)
685
686 *Analysis*
687 Relative quantification was performed using the blue food dye; the mass-spec calculated
688 concentration (μM) was adjusted for the sample dilution. This was then divided by the
689 concentration of the blue dye (μM) for that sample.
690 The percentage change between young and old timepoints was calculated using the
691 equation:
692 $\% \, change = \frac{O - Y}{Y} * 100$
693 Where O is the normalised concentration at the old timepoint, and Y is the normalised
694 concentration at the young timepoint. The young concentrations from all replicates were
695 compared against the old concentrations from each replicate.
696 The microbial concentration was calculated at young and old timepoints by:
697 $Microbial\ contribution = conventional\ concentration - axenic\ concentration$
698 Where the conventional concentrations from each replicate were compared against the
699 axenic concentrations for each replicate and at every timepoint.
700

701 **Supplemental table 2.** MRM transitions for the amino acids quantified

Q1 m/z	Q3 m/z	Time (msec)	Amino Acid	DP (V)	EP (V)	CE (V)	CXP (V)
166.1	120.1	50	Phe 1	30	10	15	12
132.1	86.1	50	Leu 1	36	10	23	14
132.1	86.1	50	Ile 1	40	7	15	8
150	104	50	Met 1	30	10	15	12
118.1	72.1	50	Val 1	30	10	15	12
116	70.1	50	Pro 1	30	10	15	12
182.1	136.1	50	Tyr 1	30	10	15	12
90.1	44.1	50	Ala 1	30	10	10	12
120	74.1	50	Thr 1	30	10	15	12
76	30.1	50	Gly 1	46	10	20	12
106	60	50	Ser 1	30	10	10	12
148	84	50	Glu 1	30	10	15	12
134	88	50	Asp 1	26	10	13	14
156	110.1	50	His 1	30	10	15	12
175.1	70.1	50	Arg 1	30	10	15	12
147.1	84.1	50	Lys 1	30	10	15	12
166	103	50	Phe 2	31	10	35	28
132.1	69	50	Leu 2	36	10	23	20
150	133	50	Met 2	21	10	13	8
118	55	50	Val 2	36	10	29	6
182.1	165	50	Tyr 2	46	10	19	6
120	56	50	Thr 2	86	10	23	6
106	42	50	Ser 2	31	10	31	4
148	102	50	Glu 2	21	10	15	4
134	70	50	Asp 2	36	10	25	6
156	93	50	His 2	41	10	31	8
175	116	50	Arg 2	46	10	19	6
147	130	50	Lys 2	16	10	13	6
122	76	50	Cys 1	30	10	10	15
205.1	146.1	50	Trp 1	36	10	10	23
147.1	84.1	50	Gln 1	30	10	10	15
133	74	50	Asn 1	30	10	25	25
133	116	50	Asn 2	31	10	13	8
205.1	188	50	Trp 2	41	7	15	9
147	102	50	Gln 2	31	10	19	12
132.1	69	50	Ile 2	40	7	24	9

702
703

704 **Capillary feeding (CAFÉ) assay**

705 Food consumption was measured, essentially as previously described[34], using liquid defined
706 media made without agar and, due to issues in solubility, without cholesterol. Cotton wool
707 balls were placed at the bottom of drosophila vials and saturated with water. Any excess
708 water was removed, and the vial walls were dried. 10 μL pipette tips were trimmed to
709 enable capillary tubes to extend from the end with a tight fit so they wouldn't slip.
710 Drosophila flugs were cut in half laterally, and three prepared tips were inserted through
711 the flug. The capillary tubes were prepared by loading with 2 μL of mineral oil to limit
712 evaporation, and 10 μL of liquid food, then the interface between oil and food was marked.
713 10 mated female flies were sorted into the prepared vials. Each condition had a
714 minimum of 10 vials. Additionally, a minimum of three evaporation control vials, containing
715 no flies, were used for each experiment. Once the flies were awake within the vial, the
716 capillary tubes were inserted into the tips, so the ends extended just beyond the base of the
717 tip. The capillary tubes were changed every 24 hours, and the distance between the
718 interface between oil and food, and the mark denoting the starting interface was recorded.
719 The flies were allowed 24 hours to acclimate to the new feeding setup prior to
720 measurements being recorded. Following acclimation, the assay was performed for 24-48
721 hours. Food consumption was calculated in mm, by calculating the difference in the start
722 and end interface and subtracting the average difference in the start and end interface of
723 the evaporation controls. A conversion factor (X μL/mm) was calculated for each capillary
724 tube by dividing 10 (the amount of liquid food), by the starting interface (mm). This was
725 then used to convert food consumption in mm to μL.

726

727 **Bacterial DNA extraction**

728 30 whole flies were sorted under light CO_2 anaesthesia into microcentrifuge tubes and
729 frozen at -80 °C. Flies were then surface sterilised in 70 % ethanol for 5 minutes and rinsed
730 twice in sterile PBS. 5 flies were sorted into sterile microcentrifuge tubes and homogenised
731 in 200 µl lysis buffer (1 X TE, 1 % Triton X-100, 1/100 proteinase K (NEB, P8107S)) using a
732 mechanical pestle, with a further 300 µl of lysis buffer being added after homogenisation.
733 Lysate was incubated for 1.5 hours at 55 °C then transferred to screw cap vials containing
734 0.4 g sterilised low binding 100-micron silica beads (OPS Diagnostics, BLBG 100-200-11) and

735 vortexed for 10 minutes at max speed. Lysate was then transferred back to the original tube
736 and incubated for a further 1.5 hours at 55 °C followed by 10 minutes at 95 °C.
737
738 **RNA extraction**
739 Total RNA was extracted from 5 midguts per biological replicate. Midguts were dissected in
740 ice-cold PBS and included the cardia and midgut, through to the midgut-hindgut junction,
741 excluding the hindgut and Malpighian tubules. Midguts were homogenised in 100 µL
742 TRIzol™ (Thermofisher, 15596026) using a motorised pestle. RNA was extracted following
743 the standard TRIzol protocol.
744
745 **cDNA preparation**
746 For a 10 µL reaction, 1 µL DNase buffer (Thermo, EN0521) and 0.5 µL DNase 1 (Thermo,
747 EN0521) were added to 8.5 µL RNA solution and incubated for 30 minutes at 37 °C, to
748 remove any DNA contaminants. The DNase enzyme was then deactivated by the addition of
749 0.5 µL 50mM EDTA (Thermo, EN0521) and subsequent incubation for 10 minutes at 65 °C.
750 cDNA synthesis was carried out using Thermo Scientific's First Strand cDNA Synthesis kit. In
751 short, 1 µL of random hexamers (Thermo, SO142) were added and the samples were
752 incubated at 70 °C for 5 minutes before a 9 µL of a master mix containing 4 µL first strand
753 buffer (Thermo, EPO442), 0.5 µL RIbolock RNase inhibitor (Thermo, EO0382), 2 µL 10mM
754 dNTPs (Thermo, R0181), 0.2 µL RevertAid reverse transcriptase (Thermo, EPO442) and 2.3
755 µL molecular grade water (Sigma, W4502) per well, was added. The samples were then
756 incubated for 10 minutes at room temperature, followed by 1 hour at 37 °C and 10 minutes
757 at 70 °C. The samples were spun following each incubation step.
758
759 **Quantitative PCR**
760 qPCR was performed with Power SYBR™ Green master mix (Fisher, 10219284) on a Bio-RAD
761 CFX Connect Real-Time PCR detection system. Either 4.5 µL bacterial DNA or 1 µL of
762 *Drosophila* cDNA sample was used in a 10 µL reaction with 5 µL of Power SYBR™ Green and
763 0.5 µL of L + R primer mix. Any remaining volume was made up with molecular grade water.
764 Cycling conditions were: 95°C for 10 minutes, then 40 cycles of 95°C for 15 seconds followed
765 by 60°C for 60 seconds. All calculated gene expression values were normalised to the value

766 of the housekeeping gene rp49. Levels of the bacterial 16S rRNA gene were normalised to
767 the level of the *Drosophila* Actin gene. The primer sequences used are given in table 1.
768
769 Table 1: Primer sequences

Target	Forward primer	Reverse primer	Reference
Actin 5C	TTGTCTGGGCAAGAGGATCAG	ACCACTCGCACTTGCACTTTC	[7]
CG1698	CCAGGCGTATGTGGGTTCATT	AGAGAGCGTCTTCTTGCCATT	This study
CG43693	CCGTTGGTAATCTCTCGGAAAA	AGCGATCCCTTTAGCAAGTGT	This study
CG5535	TTATCCGCCTTCGATCTTACCG	CGGCATATTGCTTGGACACTT	This study
CG7255	CGGCAGTGTCTCAAAGTCG	TGGCGAACCATTGTTCAGTAT	This study
CG8785	AATGACTTCAACTCGAAAGCCA	GCTCGAAGGGATGGTAGGGA	This study
DmGlut	CGCCAATTAGTACCGAGATGA	CGCTGGGGTATCACGAAAT	This study
Eaat1	ATTGTGCCGCTTTTGGTCTCA	GTAATGGCTCTGGTAGCAATCTT	This study
Kazachoc (kcc)	GCCGTGGAAATCGTATTGAC	AGCGTCCTTGGTGAAGTCC	This study
NAAT1	CTTATGGGTTTGGTCTACGTTACA	CAGACCATAAACCCACACGA	This study
Minidiscs (mnd)	TGTGCCCTCGCTGATATTC	CCACGTAGCTGACGTAGTTGA	This study
Pathetic (path)	ATGTGCTCCGGTCTCATCAT	CTTGTGTCCGCATTTTACCA	This study
Rp49	ATCGGTTACGGATCGAACAA	GACAATCTCCTTGCGCTTCT	This study
Slimfast (slif)	CACAGTGAACAGCTACACGAAGA	GGTCCAGGTTAAAGAGCATGG	This study
Sobremesa	TGGGGTGGCTTTAATTGTTGG	CAGTGCGAACCAGTAAACCG	This study
16S	AGAGTTTGATCCTGGCTCAG	CTGCTGCCTYCCGTA	[82]

770
771
772 **Statistics**
773 All Statistical analyses were performed using GraphPad Prism 9, excluding the binomial tests
774 and principal component analyses which were performed in R (Rstudio build 372, R version
775 4. 0. 3). Survival curve analysis was completed using the log-rank test in GraphPad Prism;
776 the median survival was calculated by Graph Pad Prism 8 and is an approximation to the
777 closest sampling time. Quantitative PCR data and normalised DUMP amino acid data were
778 cleaned in GraphPad Prism, with outliers detected using the Robust regression and outlier
779 removal (ROUT) method with Q=1. Normality of the cleaned data was tested by Shapiro-
780 Wilk tests to determine the most appropriate statistical test. Differences between two
781 points were analysed by students t-test, or mann-whitney tests for normally and non-
782 normally distributed data respectively. Differences in gene expression values between more
783 than two time points, within or between conditions, were analysed by *two way Anova with*
784 *Tukeys multiple comparison.* P-values less than 0.05 were considered statistically significant.
785 Bar-graph error bars depict ± standard error of the mean (SEM). For all box-plots shown,

786 boxes display the 25-75th percentiles, with the horizontal bar at the median, and whiskers
787 extending from the minimum to maximum points.
788

789 **Acknowledgements**

790 We thank L. Partridge, D. Walker, and the *Drosophila* stock center (Bloomington) for fly
791 stocks, H. Siddle for technical support, the glass workshop at Durham University for
792 providing collection vials, Jeanette Alcaraz, Anona Galbraith and Sophie Waldron for helpful
793 discussions. This work was supported by the BBSRC doctoral training program and Durham
794 University. Stocks obtained from the Bloomington Drosophila Stock Center (NIH
795 P40OD018537) were used in this study.
796

797 **References**

798 1. Choi, N.-H., Kim, J.-G., Yang, D.-J., Kim, Y.-S. & Yoo, M.-A. Age-related changes in
799 Drosophila midgut are associated with PVF2, a PDGF/VEGF-like growth factor. *Aging Cell*
800 **7**, 318–334 (2008).
801 2. Biteau, B., Hochmuth, C. E. & Jasper, H. JNK activity in somatic stem cells causes loss of
802 tissue homeostasis in the aging Drosophila gut. *Cell Stem Cell* **3**, 442–455 (2008).
803 3. Li, H., Qi, Y. & Jasper, H. Preventing Age-Related Decline of Gut Compartmentalization
804 Limits Microbiota Dysbiosis and Extends Lifespan. *Cell Host Microbe* **19**, 240–253 (2016).
805 4. He, D. *et al.* Gut stem cell aging is driven by mTORC1 via a p38 MAPK-p53 pathway. *Nat*
806 *Commun* **11**, 37 (2020).
807 5. Pentinmikko, N. *et al.* Paneth cell produced Notum attenuates regeneration of aged
808 intestinal epithelium. *Nature* **571**, 398–402 (2019).
809 6. Guo, L., Karpac, J., Tran, S. L. & Jasper, H. PGRP-SC2 promotes gut immune homeostasis
810 to limit commensal dysbiosis and extend lifespan. *Cell* **156**, 109–122 (2014).
811 7. Clark, R. I. *et al.* Distinct Shifts in Microbiota Composition during Drosophila Aging Impair
812 Intestinal Function and Drive Mortality. *Cell Rep* **12**, 1656–1667 (2015).

813 8. Thevaranjan, N. *et al.* Age-Associated Microbial Dysbiosis Promotes Intestinal
814 Permeability, Systemic Inflammation, and Macrophage Dysfunction. *Cell Host Microbe*
815 **21**, 455-466.e4 (2017).
816 9. Katz, D., Hollander, D., Said, H. M. & Dadufalza, V. Aging-associated increase in intestinal
817 permeability to polyethylene glycol 900. *Dig Dis Sci* **32**, 285–288 (1987).
818 10. Rera, M., Clark, R. I. & Walker, D. W. Intestinal barrier dysfunction links metabolic and
819 inflammatory markers of aging to death in Drosophila. *Proc Natl Acad Sci U S A* **109**,
820 21528–21533 (2012).
821 11. Tran, L. & Greenwood-Van Meerveld, B. Age-associated remodeling of the intestinal
822 epithelial barrier. *J Gerontol A Biol Sci Med Sci* **68**, 1045–1056 (2013).
823 12. Dambroise, E. *et al.* Two phases of aging separated by the Smurf transition as a public
824 path to death. *Sci Rep* **6**, 23523 (2016).
825 13. Mitchell, E. L. *et al.* Reduced Intestinal Motility, Mucosal Barrier Function, and
826 Inflammation in Aged Monkeys. *J Nutr Health Aging* **21**, 354–361 (2017).
827 14. Buchon, N., Broderick, N. A., Chakrabarti, S. & Lemaitre, B. Invasive and indigenous
828 microbiota impact intestinal stem cell activity through multiple pathways in Drosophila.
829 *Genes Dev.* **23**, 2333–2344 (2009).
830 15. Smith, P. *et al.* Regulation of life span by the gut microbiota in the short-lived African
831 turquoise killifish. *Elife* **6**, e27014 (2017).
832 16. Onuma, T. *et al.* Recognition of commensal bacterial peptidoglycans defines Drosophila
833 gut homeostasis and lifespan. *PLOS Genetics* **19**, e1010709 (2023).
834 17. Salazar, A. M. *et al.* Intestinal Snakeskin Limits Microbial Dysbiosis during Aging and
835 Promotes Longevity. *iScience* **9**, 229–243 (2018).

836 18. Resnik-Docampo, M. *et al.* Keeping it tight: The relationship between bacterial dysbiosis,
837 septate junctions, and the intestinal barrier in Drosophila. *Fly (Austin)* **12**, 34–40 (2018).
838 19. Zhu, Y. *et al.* Aspirin Positively Contributes to Drosophila Intestinal Homeostasis and
839 Delays Aging through Targeting Imd. *Aging Dis* **12**, 1821–1834 (2021).
840 20. Rodriguez-Fernandez, I. A., Qi, Y. & Jasper, H. Loss of a proteostatic checkpoint in
841 intestinal stem cells contributes to age-related epithelial dysfunction. *Nat Commun* **10**,
842 1050 (2019).
843 21. Wang, L., Ryoo, H. D., Qi, Y. & Jasper, H. PERK Limits Drosophila Lifespan by Promoting
844 Intestinal Stem Cell Proliferation in Response to ER Stress. *PLoS Genet* **11**, e1005220
845 (2015).
846 22. Longo, V. D. & Anderson, R. M. Nutrition, longevity and disease: from molecular
847 mechanisms to interventions. *Cell* **185**, 1455–1470 (2022).
848 23. Wickramasinghe, K., Mathers, J. C., Wopereis, S., Marsman, D. S. & Griffiths, J. C. From
849 lifespan to healthspan: the role of nutrition in healthy ageing. *J Nutr Sci* **9**, e33 (2020).
850 24. Vinardell, M. P. Age influences on amino acid intestinal transport. *Comp Biochem Physiol*
851 *Comp Physiol* **103**, 169–171 (1992).
852 25. Ferraris, R. P., Hsiao, J., Hernandez, R. & Hirayama, B. Site density of mouse intestinal
853 glucose transporters declines with age. *Am J Physiol* **264**, G285-293 (1993).
854 26. Ferraris, R. P. & Vinnakota, R. R. Regulation of intestinal nutrient transport is impaired in
855 aged mice. *J Nutr* **123**, 502–511 (1993).
856 27. Tatge, L., Solano Fonseca, R. & Douglas, P. M. A framework for intestinal barrier
857 dysfunction in aging. *Nat Aging* 1–3 (2023).
858 28. Mihaylova, M. M. *et al.* When a calorie is not just a calorie: Diet quality and timing as
859 mediators of metabolism and healthy aging. *Cell Metabolism* **35**, 1114–1131 (2023).

860 29. Piper, M. D. *et al.* A holidic medium for Drosophila melanogaster. *Nat Methods* **11**, 100–
861 105 (2014).
862 30. Piper, M. D. W. *et al.* Matching Dietary Amino Acid Balance to the In Silico-Translated
863 Exome Optimizes Growth and Reproduction without Cost to Lifespan. *Cell Metab* **25**,
864 1206 (2017).
865 31. Rera, M. *et al.* Modulation of longevity and tissue homeostasis by the Drosophila PGC-1
866 homolog. *Cell Metab* **14**, 623–634 (2011).
867 32. Babygirija, R. & Lamming, D. W. The regulation of healthspan and lifespan by dietary
868 amino acids. *Transl Med Aging* **5**, 17–30 (2021).
869 33. Bass, T. M. *et al.* Optimization of Dietary Restriction Protocols in Drosophila. *J Gerontol A*
870 *Biol Sci Med Sci* **62**, 1071–1081 (2007).
871 34. Ja, W. W. *et al.* Prandiology of Drosophila and the CAFE assay. *Proc Natl Acad Sci U S A*
872 **104**, 8253–8256 (2007).
873 35. Dutta, D. *et al.* Regional Cell-Specific Transcriptome Mapping Reveals Regulatory
874 Complexity in the Adult Drosophila Midgut. *Cell Rep* **12**, 346–358 (2015).
875 36. Krause, S. A., Overend, G., Dow, J. A. T. & Leader, D. P. FlyAtlas 2 in 2022: enhancements
876 to the Drosophila melanogaster expression atlas. *Nucleic Acids Res* **50**, D1010–D1015
877 (2022).
878 37. Hu, Y. *et al.* An integrative approach to ortholog prediction for disease-focused and
879 other functional studies. *BMC Bioinformatics* **12**, 357 (2011).
880 38. Hu, Y. *et al.* FlyRNAi.org-the database of the Drosophila RNAi screening center and
881 transgenic RNAi project: 2021 update. *Nucleic Acids Res* **49**, D908–D915 (2021).

882 39. Goberdhan, D. C. I., Meredith, D., Boyd, C. A. R. & Wilson, C. PAT-related amino acid
883 transporters regulate growth via a novel mechanism that does not require bulk
884 transport of amino acids. *Development* **132**, 2365–2375 (2005).
885 40. Deng, H., Gerencser, A. A. & Jasper, H. Signal integration by Ca(2+) regulates intestinal
886 stem-cell activity. *Nature* **528**, 212–217 (2015).
887 41. Colombani, J. *et al.* A nutrient sensor mechanism controls Drosophila growth. *Cell* **114**,
888 739–749 (2003).
889 42. Roman, G., Endo, K., Zong, L. & Davis, R. L. P{Switch}, a system for spatial and temporal
890 control of gene expression in Drosophila melanogaster. *Proc Natl Acad Sci U S A* **98**,
891 12602–12607 (2001).
892 43. Osterwalder, T., Yoon, K. S., White, B. H. & Keshishian, H. A conditional tissue-specific
893 transgene expression system using inducible GAL4. *Proceedings of the National*
894 *Academy of Sciences of the United States of America* **98**, 12596 (2001).
895 44. Bjordal, M., Arquier, N., Kniazeff, J., Pin, J. P. & Léopold, P. Sensing of amino acids in a
896 dopaminergic circuitry promotes rejection of an incomplete diet in Drosophila. *Cell* **156**,
897 510–521 (2014).
898 45. Sun, J. *et al.* Drosophila FIT is a protein-specific satiety hormone essential for feeding
899 control. *Nat Commun* **8**, 14161 (2017).
900 46. Buchon, N., Broderick, N. A., Kuraishi, T. & Lemaitre, B. Drosophila EGFR pathway
901 coordinates stem cell proliferation and gut remodeling following infection. *BMC Biol* **8**,
902 152 (2010).
903 47. Zhai, Z., Boquete, J.-P. & Lemaitre, B. Cell-Specific Imd-NF-κB Responses Enable
904 Simultaneous Antibacterial Immunity and Intestinal Epithelial Cell Shedding upon
905 Bacterial Infection. *Immunity* **48**, 897-910.e7 (2018).

906 48. Wu, M., Xiao, H., Shao, F., Tan, B. & Hu, S. Arginine accelerates intestinal health through
907 cytokines and intestinal microbiota. *Int Immunopharmacol* **81**, 106029 (2020).
908 49. Singh, K. *et al.* Dietary Arginine Regulates Severity of Experimental Colitis and Affects the
909 Colonic Microbiome. *Front Cell Infect Microbiol* **9**, 66 (2019).
910 50. Nüse, B. & Mattner, J. L-arginine as a novel target for clinical intervention in
911 inflammatory bowel disease. *Explor Immunol.* **1**, 80–89 (2021).
912 51. Kim, Y. J. *et al.* Arginine-mediated gut microbiome remodeling promotes host
913 pulmonary immune defense against nontuberculous mycobacterial infection. *Gut*
914 *Microbes* **14**, 2073132 (2022).
915 52. Gebeyew, K., Yang, C., He, Z. & Tan, Z. Low-protein diets supplemented with methionine
916 and lysine alter the gut microbiota composition and improve the immune status of
917 growing lambs. *Appl Microbiol Biotechnol* **105**, 8393–8410 (2021).
918 53. Xiao, W. *et al.* Glutamate prevents intestinal atrophy via luminal nutrient sensing in a
919 mouse model of total parenteral nutrition. *FASEB J* **28**, 2073–2087 (2014).
920 54. Hou, Q. *et al.* Exogenous L-arginine increases intestinal stem cell function through
921 CD90+ stromal cells producing mTORC1-induced Wnt2b. *Commun Biol* **3**, 611 (2020).
922 55. Fan, X. *et al.* Rapamycin preserves gut homeostasis during Drosophila aging. *Oncotarget*
923 **6**, 35274–35283 (2015).
924 56. Schinaman, J. M., Rana, A., Ja, W. W., Clark, R. I. & Walker, D. W. Rapamycin modulates
925 tissue aging and lifespan independently of the gut microbiota in Drosophila. *Sci Rep* **9**,
926 7824 (2019).
927 57. Juricic, P. *et al.* Long-lasting geroprotection from brief rapamycin treatment in early
928 adulthood by persistently increased intestinal autophagy. *Nat Aging* **2**, 824–836 (2022).

929 58. Lu, J. *et al.* Sestrin is a key regulator of stem cell function and lifespan in response to
930 dietary amino acids. *Nat Aging* **1**, 60–72 (2021).
931 59. Na, H.-J. *et al.* Metformin inhibits age-related centrosome amplification in Drosophila
932 midgut stem cells through AKT/TOR pathway. *Mechanisms of Ageing and Development*
933 **149**, 8–18 (2015).
934 60. Tokarz, J. *et al.* Common Muscle Metabolic Signatures Highlight Arginine and Lysine
935 Metabolism as Potential Therapeutic Targets to Combat Unhealthy Aging. *Int J Mol Sci*
936 **22**, 7958 (2021).
937 61. Ma, S. *et al.* Cell culture-based profiling across mammals reveals DNA repair and
938 metabolism as determinants of species longevity. *eLife* **5**, e19130 (2016).
939 62. Wan, Q.-L. *et al.* Metabolomic signature associated with reproduction-regulated aging in
940 Caenorhabditis elegans. *Aging (Albany NY)* **9**, 447–474 (2017).
941 63. Hastings, J. *et al.* Multi-Omics and Genome-Scale Modeling Reveal a Metabolic Shift
942 During C. elegans Aging. *Frontiers in Molecular Biosciences* **6**, (2019).
943 64. Pontoizeau, C. *et al.* Metabolomics analysis uncovers that dietary restriction buffers
944 metabolic changes associated with aging in Caenorhabditis elegans. *J Proteome Res* **13**,
945 2910–2919 (2014).
946 65. Edwards, C. *et al.* Mechanisms of amino acid-mediated lifespan extension in
947 Caenorhabditis elegans. *BMC Genet* **16**, 8 (2015).
948 66. Cheng, S. *et al.* Distinct metabolomic signatures are associated with longevity in
949 humans. *Nat Commun* **6**, 6791 (2015).
950 67. Tsugawa, Y., Handa, H. & Imai, T. Arginine induces IGF-1 secretion from the endoplasmic
951 reticulum. *Biochem Biophys Res Commun* **514**, 1128–1132 (2019).

952 68. Alba-Roth, J., Müller, O. A., Schopohl, J. & Werder, K. V. Arginine Stimulates Growth
953 Hormone Secretion by Suppressing Endogenous Somatostatin Secretion. *The Journal of*
954 *Clinical Endocrinology & Metabolism* **67**, 1186–1189 (1988).
955 69. Holzenberger, M. *et al.* IGF-1 receptor regulates lifespan and resistance to oxidative
956 stress in mice. *Nature* **421**, 182–187 (2003).
957 70. Aguiar-Oliveira, M. H. & Bartke, A. Growth Hormone Deficiency: Health and Longevity.
958 *Endocrine Reviews* **40**, 575–601 (2019).
959 71. Canfield, C.-A. & Bradshaw, P. C. Amino acids in the regulation of aging and aging-
960 related diseases. *Translational Medicine of Aging* **3**, 70–89 (2019).
961 72. Carroll, B. *et al.* Control of TSC2-Rheb signaling axis by arginine regulates mTORC1
962 activity. *Elife* **5**, e11058 (2016).
963 73. Hoffman, J. M. *et al.* Effects of age, sex, and genotype on high-sensitivity metabolomic
964 profiles in the fruit fly, Drosophila melanogaster. *Aging Cell* **13**, 596–604 (2014).
965 74. Bayliak, M. M. *et al.* Dietary L-arginine accelerates pupation and promotes high protein
966 levels but induces oxidative stress and reduces fecundity and life span in Drosophila
967 melanogaster. *J Comp Physiol B* **188**, 37–55 (2018).
968 75. Govindaraju, T., Sahle, B. W., McCaffrey, T. A., McNeil, J. J. & Owen, A. J. Dietary
969 Patterns and Quality of Life in Older Adults: A Systematic Review. *Nutrients* **10**, 971
970 (2018).
971 76. Volpi, E., Mittendorfer, B., Rasmussen, B. B. & Wolfe, R. R. The response of muscle
972 protein anabolism to combined hyperaminoacidemia and glucose-induced
973 hyperinsulinemia is impaired in the elderly. *J Clin Endocrinol Metab* **85**, 4481–4490
974 (2000).

975 77. Katsanos, C. S., Kobayashi, H., Sheffield-Moore, M., Aarsland, A. & Wolfe, R. R. Aging is
976 associated with diminished accretion of muscle proteins after the ingestion of a small
977 bolus of essential amino acids2. *The American Journal of Clinical Nutrition* **82**, 1065–
978 1073 (2005).
979 78. Katsanos, C. S., Kobayashi, H., Sheffield-Moore, M., Aarsland, A. & Wolfe, R. R. A high
980 proportion of leucine is required for optimal stimulation of the rate of muscle protein
981 synthesis by essential amino acids in the elderly. *Am J Physiol Endocrinol Metab* **291**,
982 E381-387 (2006).
983 79. Kabil, H., Kabil, O., Banerjee, R., Harshman, L. G. & Pletcher, S. D. Increased
984 transsulfuration mediates longevity and dietary restriction in Drosophila. *Proc Natl Acad*
985 *Sci U S A* **108**, 16831–16836 (2011).
986 80. Lewis, E. A new standard food medium. *Drosophila Information Service* 117–118 (1960).
987 81. Bakula, M. The persistence of a microbial flora during postembryogenesis of Drosophila
988 melanogaster. *Journal of Invertebrate Pathology* **14**, 365–374 (1969).
989 82. Claesson, M. J. *et al.* Composition, variability, and temporal stability of the intestinal
990 microbiota of the elderly. *Proc Natl Acad Sci U S A* **108 Suppl 1**, 4586–4591 (2011).
991